84-1427-13375

GEOLOGICAL BRANCH
ASSESSMENT REPORT

13,375 PART 2 OF 2

ELECTROMAGNETIC AND MAGNETIC SURVEY

KIDD CREEK MINES LTD.

SALTSPRING ISLAND 1984 AEM

PROJECT # 26H19 APRIL, 1984

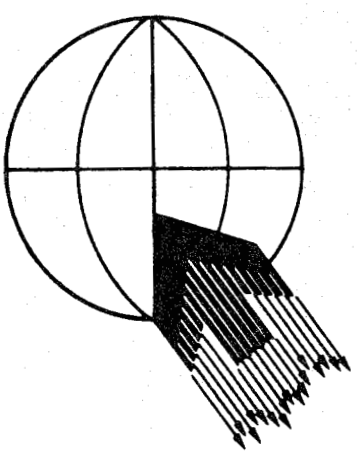

Questor Surveys Limited, 6380 Viscount Road, Mississauga, Ontario L4V 1H3

CONTENTS

1. INTRODUCTION 1

2. SURVEY OPERATIONS 2

2a. Project Location 2
2b. Production 2
2c. Survey Personnel 2
2d. Data Compilation 3

3. INPUT DATA PRESENTATION 5

4. INTERPRETATION - GENERAL 7

4a. Regional Geology 7
4b. Conductivity Analysis 7

5. INPUT INTERPRETATION 11

5.1 Salt Water Responses 11
5.2 Geological Conductivity 12
5.3 Cultural Responses 13
5.4 Weak Geological Responses 14

6. CONCLUSIONS AND RECOMMENDATIONS 22

APPENDICES

APPENDIX A BARRINGER/QUESTOR MARK VI INPUT(R) System A-1

APPENDIX B The Survey Aircraft B-1

APPENDIX C INPUT System Characteristics C-1

APPENDIX D INPUT Processing D-1

APPENDIX E INPUT Interpretation Procedures E-1

APPENCIX F INPUT Response Models F-1

APPENDIX G Quantitative Interpretation G-1

APPENDIX H Bibliography H-1

Input Survey Results ..... 1st pocket

Total Magnetic Intensity Survey ..... 2nd pocket

DATA SHEETS

LISTING OF PICKED FIDUCIAL POINTS

1. INTRODUCTION

This report contains our interpretation of the results on an INPUT MK VI airborne electromagnetic and magnetic survey flown for Kidd Creek Mines Ltd. The survey area lies within the Province of British Columbia, approximately 10 kilometres east of the Town Duncan on Vancouver Island. The area outline is presented on the following page.

The survey was commissioned by Mr. P. DeLancey of Kidd Creek Mines Ltd. on April 26, 1984. D. Martyn, Geophysicist for Questor supervised the data acquisition and preliminary data reduction while the author completed data compilation through to the completion of the project in July, 1984. Mr. G. Hendrickson of Kidd Creek Mines visited the survey base to review results and production.

The survey objective is the detection and location of base metal sulphide conductors within mostly Paleozoic volcano-sedimentary lithology of the Sicker Group.

The primary survey area consists of 214 kilometres of traverse and control lines. These were flown on June 11 and June 12, 1984 using Duncan as the survey operations base.

2. SURVEY OPERATIONS

2a. Project Location

A Bell 205A Helicopter equipped with the **QUESTOR/BARRINGER** MK VI INPUT system was utilized for the survey, which is composed of 1 contiguous block. The survey area lies at the junction of N.T.S. Maps 92B12 and 13.

2b. Production

The flight line spacing over the block was 200 metres. The table summarizes the kilometres flown during the survey operation.

Traverse lines	212	km.
Control lines	16	km.
Total lines	228	km.

The survey was completed in two production days and three flights. A further flight on June 18 was used to place fill-in lines to span navigation gaps. No production was lost to any cause during the survey.

2c. Survey Personnel

The survey crew was made up of experienced **QUESTOR** and **Trans Canada Helicopter** employees:

Crew Manager/Geophysicist	-	D. Martyn
Pilot/Captain of Helicopter	-	B. Masson (Trans Canada)
Co-Pilot/Navigator	-	B. Smith
INPUT Equipment Technician	-	D. Makos
Aircraft Engineer	-	J. Caza (Trans Canada)

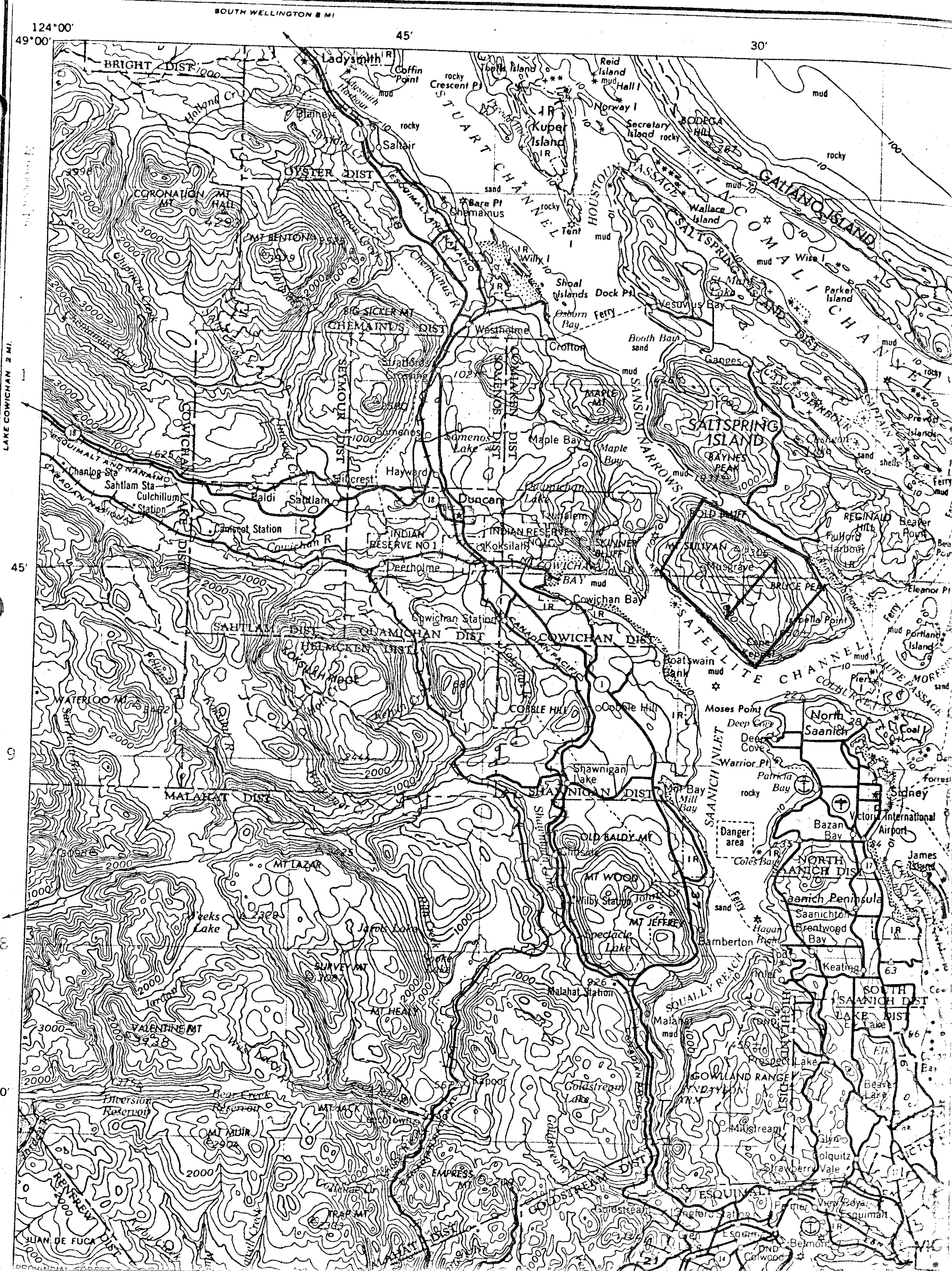

SOUTH WELLINGTON 8 MI
124°00'
49°00'
45'
30'
LAKE COWICHAN 2 MI.
PORT RENFREW 19 MI.
Ladysmith
Coffin Point
Crescent Pt
Thetis Island
Reid Island
Hall I
Norway I
Kuper Island
Secretary Island
BODEGA HILL
Saltair
STUART CHANNEL
TRINCOMALI CHANNEL
GALIANO ISLAND
HOUSTOUN PASSAGE
Wallace Island
Wise I
Parker Island
BRIGHT DIST
OYSTER DIST
CORONATION MT
MT HALL
MT BENTON
Bare Pt
Chemainus
Chemainus R
Tent I
Willy I
Shoal Islands
Dock Pt
Vesuvius Bay
Osborn Bay
Ferry
Booth Bay
Crofton
Westholme
BIG SICKER MT
CHEMAINUS DIST
SEYMOUR DIST
COMIAKEN DIST
SOMENOS DIST
Somenos
Somenos Lake
MAPLE MT
Maple Bay
SANSUM NARROWS
Ganges
SALTSPRING ISLAND
BAYNES PEAK
SALTSPRING ISLAND DIST
CAPTAIN PASSAGE
Chanlog Sta
Sahtlam Sta
Culchillum Station
Baldi
Sahtlam
Hillcrest
Hayward
Duncan
Quamichan Lake
Tzouhalem
INDIAN RESERVE NO 1
INDIAN RESERVE NO 1C
Koksilah
Cowichan R
Deerholme
SKINNER BLUFF
MT SULIVAN
Musgrave
BRUCE PEAK
Fulford Harbour
REGINALD HILL
Beaver Point
COWICHAN BAY
Cowichan Bay
Cowichan Station
COWICHAN LAKE DIST
SAHTLAM DIST
QUAMICHAN DIST
HELMCKEN DIST
COWICHAN DIST
KOKSILAH RIDGE
SATELLITE CHANNEL
Isabella Point
Cape Keppel
Boatswain Bank
Moses Point
Deep Cove
Warrior Pt
North Saanich
Patricia Bay
Sidney
Victoria International Airport
Bazan Bay
James Island
Coal I
Portland Island
MORESBY PASSAGE
COLBURNE PASSAGE
WATERLOO MT
COBBLE HILL
Cobble Hill
Shawnigan Lake
SHAWNIGAN DIST
Mill Bay
SAANICH INLET
Danger area
MALAHAT DIST
OLD BALDY MT
MT WOOD
MT LAZAR
Weeks Lake
Jacob Lake
Wilby Station
MT JEFFREY
Spectacle Lake
Coles Bay
NORTH SAANICH DIST
Saanich Peninsula
Saanichton
Brentwood Bay
Bamberton
Hagan Bight
Keating
SURVEY MT
Malahat Station
SQUALLY REACH
SOUTH SAANICH DIST
LAKE DIST
MT HEALY
VALENTINE MT
Malahat
Prospect Lake
GOWLAND RANGE
Goldstream Lake
Kapoor
Diversion Reservoir
Bear Creek Reservoir
MT JACK
MT MUIR
Millstream
Glyn
Colquitz
Strawberry Vale
EMPRESS MT
TRAP MT
GOLDSTREAM DIST
ESQUIMALT
Goldstream
Langford Station
View Royal
Esquimalt
RENFREW DIST
JUAN DE FUCA DIST
Colwood

The flight path recovery was completed at the survey base, while the final data compilation and drafting was carried out by QUESTOR at its Mississauga, Ontario office. The magnetic and electromagnetic processing was carried out using QUESTOR software and computer drafted by DATAPLOTTING SERVICES. The INPUT interpretation and reporting was completed by M.H. Konings, P.Eng.

Mr. Grant Hendrickson, Geophysicist for Kidd Creek Mines was the technical authority for the project. A preliminary compilation of results - a red ball anomaly map - was kept current at the survey base and presented to Kidd Creek Mines at the completion of the field data acquisition.

2d. Data Compilation

The flight path of the aircraft is recorded by a frame camera on black and white 35 mm. film continuously during flight. The camera is controlled by the fiducial time system of the data acquisition system so that pictures are taken once every 2 seconds. Fiducial numbers are imprinted on the film, marked onto the analogue records and recorded digitally at the same instant.

The flight line headings are opposite on adjacent lines, which are normally flown sequentially in an "S" pattern. The navigation references are flight strips at a scale of 1:20,000 which are made from the base maps. The equipment operator logs the flight details recording line numbers, time, the fiducial range and other pertinent flight information. This information comes from the magnetic tape after it has been recorded (read-

after-write). It is compared to the film, analogue records and the magnetic base station recording at the completion of the survey flight.

The film and all records are developed, edited and checked at the completion of each flight. Recovery of the flight track is carried out by comparing the negative of the 35 mm. film to the topographic features of the base map. Coincident features are picked and plotted on exact copies of the stable mosaic base map on which the final results are drafted. Points are picked at an average interval of 1 kilometre. This corresponds to one whole fiducial unit or 20 seconds. The picked points will not necessarily fall on whole fiducial numbers, but on the final presentation, only the first and last whole numbers on a line are marked on each flight line. By interpolation, the whole numbers are marked as ticks along the flight path. This keeps the anomaly and interpretation maps free of unnecessary numbers. The actual location of the picked fiducials is marked on the flight path as a round point, whose fiducial value is summarized at the end of this report.

These procedures are performed daily so that the data quality and progress may be measured objectively. Reflights for covering navigational gaps and other deficiencies are usually flown on the following day.

The analogue records are inspected for coherence with specifications, and anomalies are selected for classification and plotting. Selected anomalous conductors are positioned by

plotting their fiducial positions, less the lag factor (Appendix C). These resultant positions are located by interpolating between fiducial points established by the flight path recovery process.

The survey results are presented as 4 products. There is an INPUT anomaly map with magnetic contours, a magnetic contour overlay with flight lines and an E.M. anomaly map with interpretation.. The summary describes the interpretation of INPUT results and presents recommendations for ground follow-up surveys. In addition, a colour contour map is also provided.

3. INPUT DATA PRESENTATION

The base maps for the survey area are photomosaics constructed from 1:63,350 air photographs supplied by the British Columbia Map Office and taken in 1982. These were used first for the flight strips and later as the base onto which the flight path was recovered. The mosaics are uncontrolled at a scale of 1:10,000. The area was partitioned as illustrated on the location map.

The INPUT anomaly map presents the information extracted from the analogue records. This consists chiefly of the peak anomaly positions and response characteristrics, surficial responses, up-dip responses, and magnetic anomaly locations. In effect, these represent the primary data analysis. The symbols are explained in the map legend, but the following observations are presented:

- position of peak anomaly;
- conductance or conductivity-thickness;
- amplitude of channel 2 response;
- channel 2 half amplitude profile width (for amplitudes greater than 75 ppm);
- position and peak amplitude of associated magnetic anomalies;
- where present, surficial, up-dip, poorly defined responses have been identified with a unique symbol.

The INPUT interpretation maps outline the geophysical-geological interpretation of the electromagnetic, magnetic, geological and physiographic data. The primary survey target - bedrock conductors have axis locations and dip directions, where they are interpretable. The anomalous zones which are recommended for follow-up have a reference label assigned, to which additional comments and recommendations are directed in the Interpretation Report, following this section. Surficial response sources are mapped out by boundaries showing their interpreted lateral extent. The following list summarizes the interpretation presentation:

- bedrock conductor axis, probable and possible;
- conductor dip;
- surficial conductor outlines;
- anomalous conductors selected for ground evaluation with reference number.

4. INTERPRETATION - GENERAL

4a. Regional Geology

Saltspring Island is underlain by mostly Paleozoic age volcanic and sedimentary rocks of the Sicker Group. The exposure of these older units in Southern Vancouver Island occurred as a result of an event described as the Cowichan-Horne Lake Uplift. Younger Mesozoic rocks of the Nanaimo Group have been reported to directly overlie rocks of the Sicker Group. These are exposed at the Sansum Narrows and at the southeast corner of the island.

Specifically, the survey area is dominated by the Myra Formaation. These are described by J.E. Muller in GSC Paper 79-30 as a thick succession of schistose, folded and deformed rocks. The rocks have apparently been derived from basic to silicic tuff and breccia with some argillite and greywacke.

It has been reported that sills of meta diabase are intercalated with the sediments. On early geological references, the Sicker Group appears to have been mapped as the "Saanich Granodiorite". The Saltspring Intrusive in the northern half of Saltspring Island has been interpreted as the lower level of a volcanic centre in the reference. The economic of the Myra Formation is demonstrated by the Ag, Au, Cu, Pb, Zn and Cd mineralization in the Westmin Deposits, presently being mined.

4b. Conductivity Analysis

The conductivity-thickness products of planar horizontal and thin, steeply dipping conductors are proportional to the time constant of the secondary field electromagnetic transient decay. This transient may be closely approximated by an exponential

function for which the conductivity-thickness product (TCP) is inversely proportional to the log difference of two channel amplitudes at their respective sample times.

These response functions are presented in the form of graphs in which the amplitudes of the 6 channels of INPUT response are plotted on a logarithmic scale against conductivity. The relative amplitudes of the secondary response, at any given conductivity, may be accurately related to the depth of a conductor below the surface. These are typically referred to as Palacky nomograms. These are available for a number of conductor geometries. It has been found that the shape of the decay transient and its amplitude is usually unique to a particular geometry. Therefore, if the origin of a conductive response is in question, a good "fit" of the peak response amplitude to one nomogram will define its origin.

The 90^{o} nomogram was utilized exclusively to determine the apparent conductances of the responses obtained from the survey. This assumption is valid for near vertical conductors, within a dip range or $45\text{-}135^{o}$, relative to the aircraft flight direction.

Although the conductor depth can be interpreted from the nomograms, the short strike lengths and the variability of conductor geometry may result in the over-estimation of depths. The response shapes are indicative of shallow depth conductors over the entire survey area, with 0-50 metre depths interpreted for most selected zones. The INPUT system depth capability is typically 200 metres for a vertical, 600 metre strike length by 300 metre depth extent target. The effective penetration depth

increases for a dipping target and decreases for a smaller size conductor.

Depths were only determined for responses which appear to fit the interpretation model - a thin near vertical plate with a strike length of greater than 500 metres. Qualifications for these determinations are summarized in the interpretation section.

An anomaly listing at the back of this report summarizes each anomalous response in a numerical sequence. In addition to the standard anomaly parameters, an "anomaly type" classification has been added. The letters correlate with the plotted symbols according to the following table.

ANOMALY TYPE	RESPONSE SOURCE	SYMBOL
BLANK	bedrock conductors	circular
S	surficial (overburden or lakebottom) conductivity	diamond
U	up-dip accessory peak to main response	half circular, half diamond, symbolically "pointing" in dip direction
W	down-dip peak	same as above
P	poorly defined response	asterisk "*" in lower left quadrant
C	cultural source	square

The "P" poorly defined response may not yield signatures diagnostic of a discrete bedrock anomaly to standard electromagnetic prospecting equipment. Interpreted axis locations may be approximate for these intercepts.

5. INPUT INTERPRETATION

Above background electromagnetic responses of the Saltspring Island INPUT survey can be categorized into five classes:

a) salt water conductivity - Satellite and Sansum Narrows;

b) geological conductivity enhanced with probable electrolytic solutions (salt water);

c) cultural responses;

d) weak geological responses;

e) bedrock responses.

In addition to the above, a uniform background secondary field was evident over almost all of the survey. This is undoubtedly due to a very weak electrolytic conduction in soils caused by salt on Channels 1 and 2 as a very fast decay, however it is much stronger in the perimeter of the amplitudes of the survey area, close to the water level. The half width amplitudes of channel 1 are very broad and extend well inland for the salt water responses. This can be attributed to higher concentrations of salt caused by wind-borne spray.

This has an additional effect on the conductors in the survey area. Current gathering or the effect of surficial conductivity interacting with a bedrock conductor has probably helped to enhance weak geological conductors, generally causing exaggerated response amplitudes.

5.1 Salt Water Responses

Response 10380A is typical of a salt water response contrasted to generally resistive conditions northward towards

responses B,C and D. The physical model for salt water is a horizontal layer. No shift of the channel peaks should occur, and in the absence of altimeter variations, only a single peak will be registered. Where there is no salt water intrusion, the responses will return to background levels quickly and predictably. The half width limits for horizontal conductors very accurately delineate the extent of the horizontal conductivity.

Salt water responses as a rule occur at the edge of the survey area and as a rule, the peak amplitudes occur further out, past the ends of the flight lines. From responses 10260A and 10380A, the high conductances are characteristic of a salt water response.

5.2 Geological Conductivity

Although the author had only sketchy geological information available, across the northern survey boundary a unit of the Nanaimo group of Nesozoic age sediments is in contact with the Sicker Group. We propose that the southern extent of the conductivity for those horizons marks the contact. The responses are broad and originate from a wide source. To distinguish this unit from adjacent weaker responses, they are represented with the diamond shaped symbols which we normally use with surficial or layer source conductivity.

At least three linear conductive bands can be traced across the northern end of the area. The southern half width limit should be a reliable contact marker between a resistive and

conductive (resistivity low) rock unit. For flight lines directly adjacent to Burgoyne Bay, INPUT responses for this horizon show the effects of salt water intrusion. Both amplitudes and apparent conductances increase to the west from flight line response intercepts 10340D and 10350A. This unit therefore, has both a permiability and porosity increase in contrast to the Sicker group volcanics.

Magnetic contours suggest that this unit has a marginally greater susceptibility with magnetic peaks often coincident with INPUT response peaks.

We suggest that carbonaceous sediments are the explanation for bulk conductivity where salt water intrusion is not a problem. The main evidence for this is the consistency of response shapes, response amplitudes and apparent conductances over very many kilometres.

The interpreted conductor axis represents the central portion of the conductor while the half width limits define the edges.

5.3 Cultural Responses

Where recognized, responses attributed to man made conductive sources are outlined by a black square with lower case letters. These occur between Bruce Peak and Hope Hill and extend downhill (northward) along flight lines 10221 and 10210.

The power line monitor did not respond but the shape of the responses and their positions are exactly coincident with roads. The form of the responses is a double response peak which

fits a vertical to near vertical sheet model. For cultural responses, this is usually produced by a grounded hydro or telephone line, sometimes by a fence but not by a buried pipe.

All of the responses on flight line 10221 between cultural response "A" and geological response "C" are interpreted as cultural conductivity effects, in this case seen as lateral effects from flying offset and near parallel to the source. The same principles probably apply to response 10210D.

The sharpness of ZONE 7A, combined with its location in a clearing, leaves it suspect as a bedrock source, although a film check could not confirm this. Similarly, the sharp consistent and symmetric character of ZONE 37D leaves it suspect; however, as its northern extent lies in bush, away from the potential cultural effects of Musgrave Landing, a bedrock source is possible.

5.4 Weak Geological Responses

With the notable exceptions of ZONES 7A and 37D (discussed on the following section) the southwestern third of the survey area has a resistive character. It is modified by enhanced somewhat by conductive soils; however, up to six horizons of extremely poor responses have been identified. Their generally weak character combined with wide profile widths (rarely depicted by half width presentation due to low amplitudes) leaves the interpreter to believe that these are geological units with a minor conductivity contrast. In spite of what may appear to be local conductivity-thickness anomalies caused by modification by

increasingly conductive soils in the proximity of the southwestern shore, and the author's uncertainty in classifying these responses as definitely geological to possible bedrock, no follow-up recommendations are suggested.

Two origins are possible for these horizons as depicted on the interpretation maps:

a) carbonaceous conductors;

b) permeable horizons susceptible to weathering.

The first situation is well understood; however, the second possibility would require detailed mapping to substantiate. We suggest that some of the responses could originate from within tuff horizons, for example, which could be marginally conductive by natural weathering but could also be enhanced by infiltration of natural electrolytic solutions - ground water with salt spray.

The southern third of the survey area is also characterized by flat magnetic gradients. As there are some strike discrepancies between the interpreted axial traces and magnetic contours, comparisons with geological information are recommended to either explain the observation or modify the interpretation.

INPUT E.M. Profile Map
26H19
Channel 1 Amplitude
1" = 2000 p.p.m.
Scale 1:52238

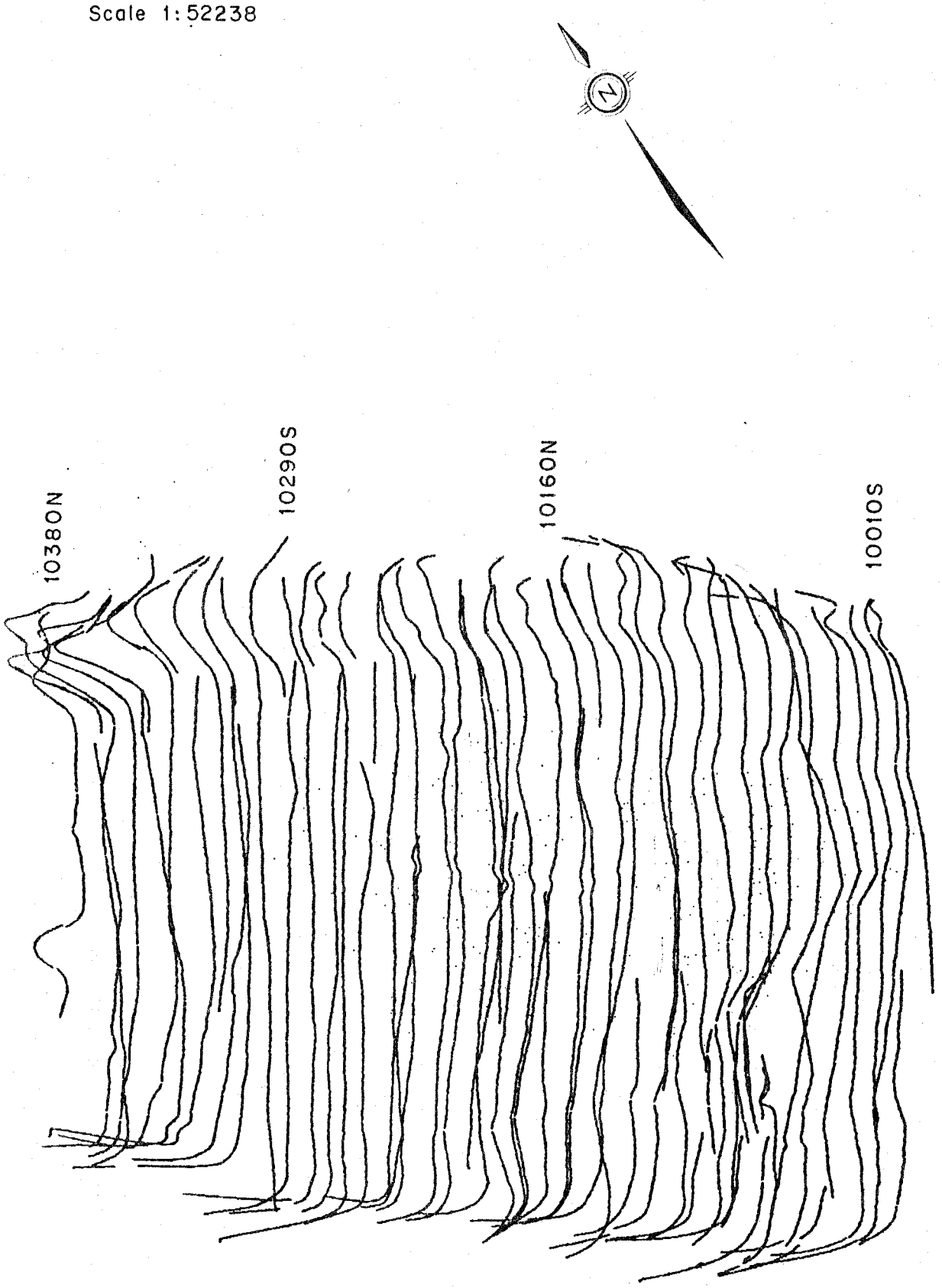

ANOMALY 1C

Conductance	14S
Dip	?
Strike Length	+ 400 m.
Magnetic Correlation	
Related Responses	10015B, 10021D, 10041D

Where the southwestern 3/4 of the survey block is characterized by a relatively flat magnetic background of 56300 nT, the area of profound formational conductors has a consistently higher background susceptibility. This may have direct relation to the Nanaimo unit. The responses selected appear to lie within this unit if there is a direct geological relation to the weak susceptibility contrast. The INPUT responses can best be described as subtle inflections on the flank of the formational conductors. It is conceivable that both the amplitudes and conductances are enhanced by the superposition of high amplitude formational responses.

The formational conductor to the north appears to dip to the northeast on flight lines 10010S and 10015S while immediately to the south, bedrock conductors dip south with no indication for the 1C response.

The axis location for the selected "anomaly" must be considered approximate; however, the vertical axis peaks should closely approximate a location over the conductive sheet if it is dipping.

ANOMALY 5B

Conductance	13S
Dip	-
Strike Length	-
Magnetic Correlation	-
Related Responses	-

The 10050B intercept is located closely adjacent to the Nanaimo unit formational conductors. The response was selected for its sharp, narrow profile. It is possible that the conductor may extend westward, superimposed on the flanks of the formational zone. The axis position should be considered approximate while its position close to a sharp local magnetic response in an otherwise uniform unit is a favourable situation.

ANOMALY 6C

Conductance Range	6-11S
Dip	S
Strike Length	3 km.
Magnetic Correlation	-
Related Responses	10010DE, 10015C, 10021C, 10030B 10041C, 10050C, 10060E (10065C)

The zone is a consistent long horizon, invarient in amplitude and conductance. The responses, except for 10010D, are up and down dip peaks, interpreted from the shifted peaks. The value of the dips is interpreted to lie between 40 and 60°. The selected response (intercept 10065C) exemplifies the form of the responses. The horizon should be investigated together with ZONE 6D (10060D), as it has no apparent section of enhanced responses.

ANOMALY 6D

Conductance	22S
Dip	S
Strike Length	400 m.
Magnetic Correlation	14 nT
Related Responses	10050D

The 6C ZONE is unique in the survey area because a magnetic anomaly is coincident with the best part of the E.M. responses. Along strike, weak and diffuse responses can be traced along strike to the NE for 2 km.; however, axis positions should only be considered approximate. The half width extent to the southwest gives a better indication of the lateral extent of the conductor, which at best is still weak and diffuse. The low amplitudes are evidence of a non-massive source of the conductivity while the "22" Siemen value presented may be somewhat artificial due to superposition with the adjacent conductive horizon to the north.

The dip of the conductor is southwest at a flat to moderate value. This is deduced by the shift of later time channel peaks in the direction of dip.

A high priority ground follow-up is recommended for this zone, utilizing techniques sensitive to poor conductors.

ANOMALY 7A

Conductance	9S
Dip	-
Strike Length	250 m.
Magnetic Correlation	-
Related Responses	10071A

Two unusually sharp responses occur isolated from other conductance trends. The sharpness and single intercept nature of the responses can only be interpreted as a limited dimension horizontal source. The responses occur in a clearing. In ground follow-up, look for a fence with or without a ground, having side lengths of less than 200 x 200 metres.

If culture cannot explain the source, then a horizontal or very flat dipping bedrock source with very limited surface projection dimensions will be the conductivity explanation. The half width shown for the 10071A response graphically presents the approximate width dimension.

ANOMALY 13F

Conductance	8S
Dip	N?
Strike Length	100 m.
Magnetic Correlation	15 NT
Related Responses	-

The 13F response intercept is weak in amplitude; however, the form of the transient suggests that the conductance has been underestimated. The response is directly associated with a local sharp magnetic peak.

The poor amplitudes, combined with the sharp response profile, are not unusual for a source with limited dimensions and this type of response is associated with spheric or system noise characteristics.

The response, in spite of its limited dimensions, should be considered a first priority target.

ANOMALY 37D

Conductance	34S
Dip	90°
Strike Length	+ 1,100 m.
Magnetic Correlation	-
Related Responses	10331DE, 10340AB, 10351BC, 10360AB, 10365AB, 10371C

All of ZONE 37D responses are typical of a vertical sheet target. The higher amplitudes of the western intercepts (ie, 10331E, 10340A) relative to their matching responses on the opposite side of the conductor axis can be attributed to superposition of background resistivity low responses. The exceptional consistency of the response shapes and amplitudes is often a sign of culture. Although the responses do trend through some open areas near Musgrave Landing, they also extend northward into an area of thick bush.

If the zone has a cultural source then the low amplitudes would be attributed to a vertical ribbon type conductor. No depth interpretation was attempted for this zone as the low amplitudes would cause an overestimate of depth for a conductor whose shape is characteristic of a shallow source.

6. CONCLUSIONS AND RECOMMENDATIONS

Although surficial conductivity is present in the survey area, it is homogenous in nature and does not severely interfere with the INPUT interpretations with the exception of the presented half width extent. These may be locally overestimated, especially in coastal areas to the southwest.

Formational conductors, with the exception of the strong zone along the northeast survey boundary, may be supplemented with representative sections of the weaker horizons and the "isolated" responses which occur randomly throughout the project area, for which no axis interpretation has been made. The model targets for the survey - the Westmin Deposits - are not noted for electrical characteristics, especially when depths are well below the ground surface and the target size is finite.

Respectfully submitted,

QUESTOR SURVEYS LIMITED

Marcel H. Konings, P.Eng.,
Senior Geophysicist.

JOB NO:26N19

INPUT EM LINE	FIDUCIAL	ANOMALY TYPE	CHS	PEAK RESPONSE AMPLITUDES (PPM) CH1	CH2	CH3	CH4	CH5	CH6	TCP (S)	ALT (M)	MAGNETIC FIDUCIAL	VALUE
19020A	21.593	P	2	193	116	-	-	-	-	NC	148	-	
19020B	22.245	P	3	158	104	58	-	-	-	8	146	-	
19020C	27.794	S	3	328	173	91	-	-	-	7	146	-	
19020D	29.481	S	2	286	143	-	-	-	-	NC	147	-	
19010A	11.165	S	5	237	163	104	63	37	-	32	153	-	
19010B	13.648	S	2	212	92	-	-	-	-	NC	136	-	
19010C	17.274	P	3	118	74	46	-	-	-	11	151	-	
19010D	19.453	P	4	149	104	68	39	-	-	29	145	-	
10010A	138.193	U	6	684	441	260	150	91	54	27	151	-	
10010B	138.567		6	544	303	159	85	45	19	17	142	138.73	23
10010C	138.954		5	227	123	68	28	13	-	14	119	-	
10010D	139.716	P	3	143	67	31	-	-	-	9	129	-	
10010E	140.170	P	3	202	92	31	-	-	-	6	127	140.20	12
10011A	143.865	S	2	104	25	-	-	-	-	NC	127	-	
10011B	144.610	S	3	194	60	11	-	-	-	3	145	-	
10015A	49.939	U	6	629	383	218	118	64	33	21	148	-	
10015B	50.461	P	5	269	159	86	49	32	-	19	135	-	
10015C	51.782	P	2	223	95	-	-	-	-	NC	133	52.60	25
10015D	55.471	S	2	125	39	-	-	-	-	NC	136	-	
10015E	56.540	S	3	214	79	34	-	-	-	8	133	-	
10021A	130.037	S	2	143	60	-	-	-	-	NC	131	-	
10021B	130.866	S	3	179	75	25	-	-	-	6	118	-	
10021C	135.603	P	3	199	82	29	-	-	-	6	122	134.70	30
10021D	136.692	P	4	138	83	40	19	-	-	11	119	136.90	17
10021E	137.500	S	6	538	312	170	94	45	22	19	145	-	
10030A	116.305	S	6	627	327	172	85	49	21	17	143	116.70	40
10030B	118.144	P	3	194	81	31	-	-	-	7	139	-	
10030C	123.238	P	3	184	61	29	-	-	-	10	134	-	
10030D	124.147	S	3	148	44	20	-	-	-	9	135	-	
10030E	125.695	S	4	246	132	68	40	-	-	14	143	-	
10041A	107.391	S	2	138	62	-	-	-	-	NC	147	-	
10041B	108.212	S	2	184	57	-	-	-	-	NC	123	-	
10041C	113.757	P	3	200	75	40	-	-	-	6	130	-	
10041D	114.694	P	3	159	88	51	-	-	-	7	125	114.82	46
10041E	115.397	S	6	582	311	167	89	46	21	18	139	-	

JOB NO:26H19

INPUT EM LINE	FIDUCIAL	ANOMALY TYPE	CHS	PEAK CH1	RESPONSE CH2	AMPLITUDES CH3	(PPM) CH4	CH5	CH6	TCP (S)	ALT (M)	MAGNETIC FIDUCIAL	VALUE
10050A	92.871	S	6	567	299	160	80	44	25	18	117	-	
10050B	93.246	P	4	260	132	63	41	-	-	13	142	93.50	35
10050C	94.723	P	3	185	76	40	-	-	-	5	126	94.88	14
10050D	94.996	P	3	201	79	32	-	-	-	8	126	-	
10050E	101.289	P	2	140	41	-	-	-	-	NC	123	-	
10050F	101.904	S	2	216	49	-	-	-	-	NC	111	-	
10050G	102.888	S	3	231	96	43	-	-	-	9	130	-	
10060A	81.506	S	6	469	215	126	62	34	18	21	141	-	
10060B	82.596	S	3	225	102	41	-	-	-	8	126	-	
10060C	83.294	P	2	192	43	-	-	-	-	NC	110	-	
10060D	89.629	P	4	145	79	46	30	-	-	22	146	-	
10060E	89.915	P	3	172	76	38	-	-	-	11	119	-	
10060F	91.640	S	6	614	336	178	95	54	36	20	139	91.07	41
10065A	43.212		1	88	-	-	-	-	-	NC	146	-	
10065B	46.897	P	4	201	95	45	23	-	-	11	145	-	
10065C	47.213	P	3	258	115	45	-	-	-	7	142	-	
10065D	49.203	S	6	467	263	147	79	47	28	22	147	48.67	33
10070A	67.692	S	6	1979	1425	933	587	370	212	44	144	-	
10070B	68.213	S	6	644	355	188	100	54	26	18	145	-	
10070C	70.389	W	3	214	88	44	-	-	-	6	124	-	
10070D	74.209	P	2	103	39	-	-	-	-	NC	117	-	
10071A	77.617		3	275	81	30	-	-	-	7	135	-	
10071B	78.998	S	3	221	87	34	-	-	-	7	123	-	
10071C	79.776	S	4	436	198	104	51	-	-	13	131	-	
10075A	60.699	P	2	91	36	-	-	-	-	NC	118	-	
10075B	62.908	S	3	173	74	31	-	-	-	8	132	-	
10076A	65.578	S	3	408	179	89	-	-	-	11	113	-	
10076B	67.009	S	3	190	64	32	-	-	-	11	121	-	
10077A	68.407		4	133	41	18	8	-	-	9	142	-	
10080A	58.899	S	3	231	102	52	-	-	-	6	117	-	
10080B	59.396	S	3	192	78	42	-	-	-	8	127	-	
10081A	61.585	P	3	122	44	24	-	-	-	5	125	-	

JOB NO:26H19

LINE	INPUT EM FIDUCIAL	ANOMALY TYPE	ANOMALY CHS	PEAK RESPONSE AMPLITUDES (PPM) CH1	CH2	CH3	CH4	CH5	CH6	TCP (S)	ALT (M)	MAGNETIC FIDUCIAL	MAGNETIC VALUE
10081B	65.258	U	3	170	87	51	-	-	-	17	140	-	
10081C	67.017	S	6	509	281	155	89	53	26	22	138	-	
10090A	46.428	S	6	606	344	195	109	67	35	23	126	-	
10090B	48.810	P	3	207	94	43	-	-	-	9	125	48.67	33
10090C	49.609	P	3	157	82	52	-	-	-	11	122	-	
10090D	53.135	P	2	147	51	-	-	-	-	NC	109	-	
10090E	56.151	S	3	199	81	37	-	-	-	9	115	-	
10100A	35.471	S	3	208	95	47	-	-	-	11	123	-	
10101A	37.566	S	2	95	41	-	-	-	-	NC	133	-	
10101B	38.193	P	2	141	46	-	-	-	-	NC	126	-	
10102A	39.125	P	2	150	57	-	-	-	-	NC	134	-	
10102B	43.004	P	4	198	102	66	29	-	-	21	128	-	
10102C	43.193	P	4	210	108	67	29	-	-	18	130	-	
10102D	43.690	P	3	181	76	48	-	-	-	11	130	-	
10102E	45.124	S	5	597	306	164	92	52	-	18	132	-	
10110A	254.453	S	6	798	477	259	140	77	36	19	121	-	
10110B	254.878	S	6	494	259	142	74	39	24	20	137	-	
10110C	255.420	S	5	503	255	119	59	32	-	13	143	-	
10110D	257.242	P	3	137	53	26	-	-	-	6	134	-	
10110E	257.714	P	3	213	87	40	-	-	-	9	107	-	
10110F	258.424	P	3	103	75	29	-	-	-	7	129	-	
10110G	261.734	S	2	123	40	-	-	-	-	NC	115	-	
10111A	263.893	P	2	101	27	-	-	-	-	NC	122	-	
10111B	266.699	P	3	162	64	16	-	-	-	4	115	-	
10120A	244.099	P	3	150	56	28	-	-	-	11	117	-	
10120B	246.354	P	3	83	36	21	-	-	-	7	122	-	
10120C	247.212	P	2	120	40	-	-	-	-	NC	131	-	
10120D	250.598	P	3	146	80	35	-	-	-	9	118	-	
10120E	251.103	P	3	171	77	31	-	-	-	8	118	-	
10120F	252.908	S	6	590	304	143	69	31	10	13	128	-	
10130A	231.325	S	6	628	342	186	103	52	30	20	146	-	
10130B	231.721	S	6	554	304	162	79	44	21	17	121	-	
10130C	232.104	S	6	527	263	123	51	21	10	12	130	-	
10130D	234.115	P	3	142	54	29	-	-	-	13	130	-	
10130E	235.040	P	3	162	91	38	-	-	-	8	124	-	

JOB NO:26H19

INPUT EM LINE	FIDUCIAL	ANOMALY TYPE	CHS	PEAK RESPONSE AMPLITUDES (PPM) CH1	CH2	CH3	CH4	CH5	CH6	TCP (S)	ALT (M)	MAGNETIC FIDUCIAL	VALUE
10130F	237.889	P	3	51	37	15	-	-	-	8	113	-	
10130G	238.494	P	2	73	22	-	-	-	-	NC	116	-	
10130H	239.659	P	2	55	19	-	-	-	-	NC	120	-	
10136A	38.007	S	2	100	22	-	-	-	-	NC	120	38.42	23
10136B	38.903	S	2	92	47	-	-	-	-	NC	128	-	
10136C	40.871	P	3	177	96	55	-	-	-	11	144	-	
10140A	223.222	P	2	70	24	-	-	-	-	NC	131	-	
10140B	224.139	P	2	75	25	-	-	-	-	NC	122	-	
10140a	226.909	C											
10140C	227.900	P	4	92	66	34	23	-	-	15	138	-	
10140D	228.346	U	4	203	102	55	15	-	-	10	120	-	
10140E	228.964	P	4	148	62	31	14	-	-	12	145	-	
10140F	230.348	S	5	520	266	118	56	19	-	10	124	-	
10140G	230.803	S	6	640	348	173	87	41	21	15	138	-	
10150A	208.788	S	6	718	375	187	87	42	16	14	145	-	
10150B	209.432	S	5	479	238	115	56	22	-	12	136	-	
10151A	212.791	P	3	176	80	44	-	-	-	9	121	-	
10151a	214.485	C											
10151B	217.023		1	57	-	-	-	-	-	NC	145	-	
10151C	218.214		1	71	-	-	-	-	-	NC	122	-	
10151D	218.820		1	82	-	-	-	-	-	NC	146	-	
10160A	199.153	P	2	58	35	-	-	-	-	NC	132	-	
10160B	200.276	P	2	72	35	-	-	-	-	NC	128	-	
10160C	201.181	P	2	48	15	-	-	-	-	NC	131	-	
10160D	201.693	P	2	63	18	-	-	-	-	NC	145	-	
10160a	204.170	C											
10160E	205.900	P	4	178	82	44	12	-	-	10	118	-	
10160F	208.008	S	5	432	224	117	62	28	-	15	143	-	
10170A	187.788	S	6	733	379	196	91	50	37	17	139	-	
10170B	188.133	S	5	530	262	136	60	29	-	13	123	-	
10170C	188.479	S	4	328	156	79	39	-	-	13	142	-	
10170D	190.982	P	3	122	48	33	-	-	-	7	120	-	
10170E	191.772	P	3	149	85	45	-	-	-	9	134	-	
10170a	193.150	C											
10170F	195.693		1	64	-	-	-	-	-	NC	115	-	
10170G	196.299	P	3	74	49	25	-	-	-	12	122	-	
10170H	196.678	P	3	76	52	16	-	-	-	5	134	-	
10175a	29.019	C											

JOB NO:26H19

INPUT EM LINE	FIDUCIAL	ANOMALY TYPE	CHS	PEAK RESPONSE AMPLITUDES (PPM) CH1	CH2	CH3	CH4	CH5	CH6	TCP (S)	ALT (M)	MAGNETIC FIDUCIAL VALUE
10175A	31.517	P	3	80	35	24	-	-	-	10	122	-
10175B	31.760	P	3	86	42	22	-	-	-	12	114	-
10175C	32.391	P	3	100	54	33	-	-	-	12	124	-
10175D	33.085	P	3	102	59	45	-	-	-	12	126	-
10182A	179.190	P	3	93	31	22	-	-	-	9	120	-
10182a	183.248	C										
10182B	184.684	U	3	168	96	51	-	-	-	13	136	-
10182C	186.190		1	134	-	-	-	-	-	NC	134	-
10182D	186.994	S	5	557	284	143	62	34	-	13	131	-
10190A	155.101	S	6	586	310	166	92	49	33	20	147	-
10190B	155.492	S	5	548	290	138	61	30	-	12	132	-
10190C	158.501	S	3	99	53	21	-	-	-	7	138	-
10190a	160.063	C										
10190D	163.250	P	2	60	15	-	-	-	-	NC	130	-
10190E	164.251	P	2	60	39	-	-	-	-	NC	143	-
10191A	165.826	P	3	80	49	38	-	-	-	15	145	-
10191a	166.598	C										
10191B	169.747		1	52	-	-	-	-	-	NC	115	-
10191C	170.698	P	2	59	19	-	-	-	-	NC	125	-
10191D	171.312	P	2	80	41	-	-	-	-	NC	134	-
10200A	144.530	P	3	81	38	20	-	-	-	6	136	-
10200B	145.397	P	3	60	16	14	-	-	-	4	131	-
10200a	149.803	C										
10200C	151.997	S	2	113	37	-	-	-	-	NC	142	-
10200D	154.091	S	5	488	266	132	67	29	-	13	146	-
10200E	154.567	S	5	484	263	144	74	40	-	17	149	-
10205A	22.025	P	3	58	39	28	-	-	-	15	147	-
10205a	23.576	C										
10205B	27.435	S	6	485	276	146	77	43	23	19	148	-
10210A	131.859	S	6	1091	544	270	135	74	39	15	144	-
10210B	132.175	S	6	842	456	227	106	56	25	14	137	-
10210C	132.701	S	6	582	312	169	84	43	26	18	138	-
10210D	135.595	P	4	187	103	62	19	-	-	13	112	-
10210a	137.949	C										
10210E	141.199	P	3	55	18	11	-	-	-	6	140	-
10210F	141.889	P	3	64	32	12	-	-	-	7	135	-
10221A	120.001	S	6	1416	957	606	379	246	142	40	140	-

JOB NO:26H19

INPUT EM LINE	FIDUCIAL	ANOMALY TYPE	CHS	PEAK RESPONSE AMPLITUDES (PPM) CH1	CH2	CH3	CH4	CH5	CH6	TCP (S)	ALT (M)	MAGNETIC FIDUCIAL VALUE
10221B	121.465	P	3	96	44	37	-	-	-	12	139	-
10221a	126.251	C										
10221b	128.350	C										
10221C	130.640	S	5	527	259	136	67	34	-	15	143	-
10221D	130.993	S	6	787	428	230	116	60	34	18	144	-
10221E	131.313	S	6	894	488	259	128	72	41	18	145	-
10230A	100.875	S	6	799	411	206	103	51	19	15	126	-
10230B	101.274	S	6	689	339	177	83	38	14	14	123	-
10231a	106.354	C										
10231A	110.768	P	2	66	29	-	-	-	-	NC	118	-
10231B	111.379	P	3	72	33	8	-	-	-	4	131	-
10235a	15.893	C										
10235A	19.880	P	3	89	52	27	-	-	-	12	124	-
10235B	20.300	P	3	98	51	28	-	-	-	10	130	-
10240A	89.010	P	3	107	47	21	-	-	-	9	131	-
10240B	89.738	P	2	68	23	-	-	-	-	NC	128	-
10240a	94.947	C										
10240C	98.799	P	4	136	62	30	11	-	-	10	142	-
10240D	99.497	S	5	445	231	105	43	20	-	11	144	-
10250A	76.609	S	6	640	341	154	74	40	13	13	139	-
10250B	76.911	S	6	687	345	172	76	40	16	14	127	-
10251A	78.546	P	2	85	48	-	-	-	-	NC	156	-
10252A	86.122		1	52	-	-	-	-	-	NC	131	-
10260A	63.515	S	6	3150	2448	1289	1173	772	485	71	139	-
10260B	64.352	P	3	129	63	29	-	-	-	9	135	-
10260C	74.145	P	3	110	42	16	-	-	-	7	144	-
10260D	75.412	S	6	661	317	152	70	33	17	14	127	-
10260E	76.110	S	6	781	409	202	100	56	21	15	147	-
10270A	52.639	S	6	635	366	202	108	60	25	19	149	-
10270B	53.144	S	6	626	360	190	100	50	18	16	140	-
10271A	54.835	P	2	69	25	-	-	-	-	NC	154	-

JOB NO:26H19

INPUT EM LINE	FIDUCIAL	ANOMALY TYPE	CHS	PEAK CH1	RESPONSE CH2	CH3	AMPLITUDES CH4	CH5	(PPM) CH6	TCP (S)	ALT (M)	MAGNETIC FIDUCIAL	VALUE
10271B	62.011		1	52	-	-	-	-	-	NC	131	-	
10280A	40.691	P	3	183	100	48	-	-	-	10	140	-	
10280B	49.997	P	3	78	29	18	-	-	-	4	142	-	
10280C	50.640	P	2	116	48	-	-	-	-	NC	146	-	
10280D	50.960	P	3	175	81	45	-	-	-	10	149	-	
10280E	51.637	S	5	447	230	108	49	24	-	12	145	-	
10290A	28.888	S	4	306	170	76	41	-	-	11	149	-	
10290B	29.238	S	6	723	415	224	118	62	34	19	147	-	
10290C	29.680	S	6	772	412	221	112	57	27	17	137	-	
10292A	38.919		1	69	-	-	-	-	-	NC	134	38.42	23
10305A	20.287	P	2	86	49	-	-	-	-	NC	145	-	
10305B	21.297	S	6	719	380	181	96	48	24	15	134	-	
10305C	21.604	S	6	818	452	222	112	56	25	15	142	-	
10310A	87.100	S	6	482	236	103	45	16	14	12	146	-	
10310B	87.592	S	6	767	396	194	86	42	19	14	145	-	
10311A	92.741	P	2	30	21	-	-	-	-	NC	137	-	
10311B	94.722	P	2	30	15	-	-	-	-	NC	146	-	
10311C	95.378	P	2	41	22	-	-	-	-	NC	142	-	
10320A	62.272		3	99	46	28	-	-	-	13	140	-	
10320B	62.899	P	2	43	15	-	-	-	-	NC	133	-	
10320C	68.451	P	2	41	15	-	-	-	-	NC	133	-	
10322A	84.511	P	2	83	29	-	-	-	-	NC	151	-	
10322B	86.097	S	6	853	436	204	92	42	19	13	142	-	
10322C	86.497	S	6	620	292	143	66	36	18	14	145	-	
10330A	50.194	S	6	533	268	141	73	38	25	18	142	-	
10330B	50.631	S	6	1219	595	269	117	49	22	12	122	-	
10331A	51.934	P	3	108	59	28	-	-	-	10	155	-	
10331B	58.489	P	2	44	20	-	-	-	-	NC	127	-	
10331C	59.098	P	2	62	31	-	-	-	-	NC	134	-	
10331D	59.325		4	92	55	30	25	-	-	22	135	-	
10331E	59.645		5	266	113	60	34	18	-	17	121	-	

JOB NO:26H19

LINE	INPUT EM FIDUCIAL	ANOMALY TYPE	ANOMALY CHS	PEAK RESPONSE CH1	CH2	CH3	AMPLITUDES (PPM) CH4	CH5	CH6	TOP (S)	ALT (M)	MAGNETIC FIDUCIAL	MAGNETIC VALUE
10340A	41.285	P	4	271	122	52	31	-	-	10	137	-	
10340B	41.836	P	3	95	50	32	-	-	-	14	130	-	
10340C	48.041	P	3	96	47	15	-	-	-	6	147	-	
10340D	49.143	S	6	1295	627	275	115	51	20	11	120	-	
10340E	49.543	S	6	768	363	199	108	60	38	21	134	-	
10350A	31.593	S	5	569	349	184	94	44	-	15	144	-	
10350B	31.981	S	6	1837	1107	584	279	124	35	14	148	-	
10351A	33.455	S	3	80	48	28	-	-	-	11	161	-	
10351B	38.596		3	69	57	33	-	-	-	13	141	38.42	23
10351C	38.951		5	162	125	71	37	22	-	19	140	-	
10360A	24.820		4	121	82	51	38	-	-	34	142	-	
10360B	25.338		3	95	56	35	-	-	-	15	145	-	
10360C	29.869	S	6	1762	1349	965	676	451	314	72	150	-	
10360D	30.096	S	6	2213	1648	1103	719	439	289	50	143	-	
10360E	30.475	S	6	866	550	311	156	80	38	19	128	-	
10365A	8.797		5	143	105	73	36	19	-	31	143	-	
10365B	9.370		4	103	70	47	30	-	-	39	149	-	
10365C	14.582	S	6	1654	1083	646	344	188	97	23	149	-	
10365D	14.995	S	6	609	361	192	88	39	15	15	147	-	
10370A	15.552	S	4	253	150	80	26	-	-	11	147	-	
10370B	15.934	S	6	1337	990	694	471	323	233	67	145	-	
10370C	16.317	S	6	1833	1266	812	510	318	222	43	149	-	
10371A	17.994	P	2	58	21	-	-	-	-	NC	146	-	
10371B	20.476	P	2	61	30	-	-	-	-	NC	149	-	
10371C	21.468		4	154	89	49	23	-	-	14	133	-	
10371D	21.881		5	184	126	85	41	33	-	34	139	-	
10380A	10.356	S	6	924	696	482	323	221	159	64	146	-	
10380B	13.330	P	2	72	45	-	-	-	-	NC	142	-	
10380C	14.239	S	6	847	606	413	270	177	123	57	149	-	
10380D	14.811	S	6	779	582	421	289	209	162	79	148	-	

LINE NO.	FIDUCIAL	MAP	POSITION (INCHES) X	Y
19020	21.5	1	-2.174	20.025
19020	21.9	1	-0.890	20.126
19020	22.6	1	1.059	20.376
19020	23.0	1	2.163	20.506
19020	23.4	1	3.225	20.628
19020	23.9	1	4.543	20.874
19020	24.6	1	6.202	21.005
19020	25.1	1	7.310	20.683
19020	25.7	1	8.627	20.653
19020	26.2	1	9.958	20.630
19020	27.0	1	11.952	21.926
19020	27.2	1	12.491	22.352
19020	27.5	1	13.511	22.807
19020	27.9	1	14.920	22.875
19020	28.3	1	16.209	22.959
19020	29.2	1	18.947	22.945
19020	29.8	1	20.782	22.797
19020	30.1	1	21.777	22.499
19020	30.6	1	23.351	22.151
19020	31.0	1	24.715	21.866
19020	31.6	1	26.555	21.019
19020	32.3	1	28.755	20.275
19020	32.7	1	29.943	19.732
19020	33.5	1	32.242	18.733
19010	11.0	1	31.785	4.210
19010	11.2	1	30.960	4.213
19010	11.5	1	29.885	4.164
19010	11.8	1	28.992	4.127
19010	12.3	1	27.878	4.185
19010	12.8	1	26.426	4.351
19010	13.1	1	25.386	4.456
19010	13.5	1	24.061	4.571
19010	14.0	1	22.461	4.681
19010	14.3	1	21.480	4.784
19010	14.6	1	20.526	4.824
19010	14.9	1	19.579	4.980
19010	15.5	1	17.634	4.702
19010	15.8	1	15.978	4.437
19010	16.1	1	14.889	4.386
19010	16.4	1	13.794	4.387
19010	16.7	1	12.766	4.507
19010	16.9	1	11.677	4.387
19010	17.2	1	10.633	4.285
19010	17.6	1	9.443	4.598
19010	17.9	1	8.362	4.870
19010	18.5	1	6.488	5.368
19010	19.1	1	4.401	5.834
19010	19.4	1	3.446	6.090

LINE NO.	FIDUCIAL	MAP	POSITION (INCHES) X	Y
19010	19.8	1	2.199	6.559
19010	20.0	1	1.779	7.071
19010	20.5	1	0.799	8.316
19010	20.8	1	0.136	9.049
19010	21.2	1	-0.501	10.222
10010	138.1	1	29.358	24.848
10010	138.4	1	29.387	24.082
10010	138.7	1	29.445	23.080
10010	139.8	1	29.682	20.027
10010	140.4	1	29.866	18.149
10010	141.2	1	30.110	15.793
10010	142.1	1	30.312	13.372
10010	142.8	1	30.474	11.367
10010	143.0	1	30.526	10.852
10011	143.1	1	29.287	11.996
10011	143.5	1	29.386	10.800
10011	144.3	1	29.445	8.524
10011	145.0	1	29.617	7.158
10011	146.5	1	29.790	5.281
10011	147.2	1	29.746	3.845
10011	147.8	1	29.806	2.438
10011	147.9	1	29.815	2.159
10015	49.7	1	29.049	24.887
10015	50.1	1	29.102	23.704
10015	51.7	1	29.394	19.172
10015	52.5	1	29.556	16.922
10015	53.1	1	29.458	15.504
10015	53.9	1	29.260	13.825
10015	54.7	1	29.093	11.703
10015	55.1	1	29.080	10.652
10015	56.6	1	28.809	7.228
10015	57.2	1	28.817	5.985
10020	127.1	1	29.172	1.864
10020	127.5	1	29.114	2.715
10020	128.8	1	28.905	4.534
10020	129.0	1	28.869	4.771
10021	129.1	1	28.810	4.517
10021	130.0	1	28.784	6.452
10021	130.9	1	28.767	7.680
10021	131.6	1	28.645	9.085
10021	132.5	1	28.661	11.430
10021	133.7	1	28.563	14.038
10021	134.2	1	28.629	15.357
10021	134.7	1	28.894	16.359
10021	135.3	1	28.734	18.174
10021	136.1	1	28.519	20.322
10021	136.9	1	28.345	22.491
10021	137.7	1	28.394	24.575

LINE NO.	FIDUCIAL	MAP	POSITION (INCHES) X	Y
10030	115.9	1	27.580	25.096
10030	116.1	1	27.596	24.547
10030	117.0	1	27.802	22.455
10030	117.8	1	27.934	20.099
10030	118.3	1	28.091	18.542
10030	119.0	1	28.258	16.440
10030	119.5	1	28.353	15.340
10030	120.4	1	27.758	14.178
10030	120.8	1	27.776	13.111
10030	121.7	1	27.814	11.099
10030	122.1	1	27.798	9.950
10030	122.6	1	27.814	8.655
10030	123.7	1	28.038	6.578
10030	125.2	1	28.387	4.708
10030	125.7	1	28.603	3.704
10030	126.1	1	28.575	2.656
10030	126.4	1	28.540	1.847
10040	105.0	1	27.290	1.510
10040	105.1	1	27.291	1.740
10040	105.5	1	27.200	2.578
10040	106.4	1	27.242	4.043
10040	106.8	1	27.242	4.639
10041	106.9	1	27.246	4.050
10041	107.6	1	27.058	5.629
10041	108.4	1	27.019	6.911
10041	109.4	1	27.114	8.787
10041	109.9	1	27.265	10.133
10041	110.6	1	27.438	11.914
10041	111.0	1	27.405	13.005
10041	111.5	1	27.410	14.271
10041	112.2	1	27.794	15.359
10041	112.9	1	27.487	16.974
10041	113.3	1	27.318	17.873
10041	113.8	1	27.198	19.439
10041	114.1	1	27.146	20.429
10041	115.0	1	27.219	23.056
10041	115.6	1	27.220	24.906
10050	92.4	1	25.891	25.192
10050	92.5	1	25.912	24.989
10050	93.7	1	26.126	22.247
10050	95.3	1	26.370	17.790
10050	96.9	1	26.327	15.109
10050	97.6	1	26.289	13.654
10050	98.5	1	25.539	11.778
10050	99.0	1	25.071	10.564
10050	100.1	1	26.325	8.357
10050	101.2	1	26.184	7.096
10050	102.7	1	26.463	5.061

LINE NO.	FIDUCIAL	MAP	POSITION (INCHES) X	Y
10050	103.7	1	26.737	2.482
10050	103.9	1	26.694	1.829
10060	80.8	1	25.902	1.893
10060	80.9	1	25.866	2.075
10060	81.6	1	25.651	3.251
10060	82.0	1	25.541	4.220
10060	82.6	1	25.648	5.410
10060	83.9	1	25.637	6.799
10060	85.2	1	25.806	8.404
10060	86.0	1	26.110	10.196
10060	86.6	1	26.362	11.510
10060	87.3	1	26.633	13.349
10060	88.1	1	27.213	14.900
10060	89.2	1	26.754	17.302
10060	89.6	1	26.610	18.463
10060	90.1	1	25.852	19.975
10060	90.4	1	25.826	20.914
10060	91.0	1	25.695	22.359
10060	91.9	1	25.823	25.112
10065	42.2	1	24.234	7.056
10065	42.6	1	24.102	8.288
10065	43.2	1	23.968	10.056
10065	44.8	1	25.346	13.479
10065	45.2	1	25.387	14.413
10065	45.6	1	25.354	15.310
10065	47.2	1	25.412	19.286
10065	47.6	1	25.426	20.170
10065	48.6	1	25.590	22.280
10065	49.5	1	25.798	25.110
10070	67.6	1	25.078	25.949
10070	67.9	1	25.052	25.342
10070	68.4	1	24.907	23.775
10070	69.2	1	24.763	21.676
10070	69.8	1	24.734	20.256
10070	70.2	1	24.697	19.244
10070	71.4	1	24.662	16.669
10070	71.9	1	24.539	15.325
10070	72.5	1	24.753	13.879
10070	73.0	1	24.698	12.644
10070	73.3	1	24.714	11.868
10070	73.9	1	23.943	11.001
10070	74.4	1	23.999	9.870
10070	75.1	1	23.994	8.350
10070	76.2	1	24.357	6.651
10070	76.5	1	24.541	6.040
10071	76.7	1	24.541	9.024
10071	77.4	1	24.874	7.757
10071	78.8	1	25.327	5.760

LINE NO.	FIDUCIAL	MAP	POSITION (INCHES) X	Y
10071	79.4	1	25.538	4.227
10071	80.1	1	25.833	2.138
10071	80.3	1	25.866	1.729
10075	59.4	1	24.699	12.504
10075	60.5	1	23.797	10.087
10075	61.1	1	23.635	8.465
10075	62.2	1	23.774	6.523
10075	63.7	1	23.963	2.995
10076	64.6	1	25.240	1.574
10076	66.5	1	24.929	4.599
10076	67.0	1	24.950	5.433
10076	67.5	1	25.015	6.143
10077	68.1	1	24.639	6.738
10077	68.3	1	24.658	7.185
10077	68.7	1	24.715	8.224
10077	68.9	1	24.570	8.635
10080	57.4	1	24.035	2.098
10080	57.9	1	24.095	3.080
10080	59.2	1	24.098	5.364
10080	59.9	1	24.002	6.383
10081	60.0	1	24.208	5.936
10081	60.3	1	23.962	6.762
10081	61.1	1	23.626	8.688
10081	61.7	1	23.426	10.487
10081	62.3	1	23.961	11.829
10081	63.2	1	23.979	14.267
10081	63.8	1	24.043	15.502
10081	64.9	1	24.069	17.853
10081	65.3	1	23.949	18.775
10081	66.0	1	23.885	20.927
10081	66.5	1	23.900	22.688
10081	67.3	1	24.134	25.242
10081	67.5	1	24.126	25.762
10090	46.1	1	23.638	25.864
10090	46.6	1	23.407	24.411
10090	47.0	1	23.234	22.965
10090	47.5	1	23.066	21.528
10090	48.1	1	22.971	20.304
10090	48.9	1	22.940	18.786
10090	50.1	1	23.107	16.541
10090	50.7	1	23.233	15.287
10090	51.3	1	23.444	14.024
10090	51.8	1	23.267	12.829
10090	52.3	1	23.354	11.655
10090	52.9	1	23.037	10.013
10090	53.4	1	23.150	9.159
10090	54.2	1	23.249	7.384
10090	55.9	1	23.325	5.354

LINE NO.	FIDUCIAL	MAP	POSITION (INCHES) X	Y
10090	56.8	1	23.569	3.079
10090	57.1	1	23.707	2.205
10100	34.1	1	22.419	2.422
10100	35.5	1	22.486	4.748
10100	36.6	1	22.586	6.448
10101	36.7	1	22.981	5.496
10101	37.3	1	22.738	7.182
10101	38.0	1	22.723	8.932
10101	38.5	1	22.976	10.024
10102	38.6	1	22.595	8.304
10102	38.8	1	22.565	8.900
10102	40.1	1	22.492	11.874
10102	41.2	1	22.226	14.032
10102	42.4	1	22.231	16.749
10102	43.5	1	22.256	19.070
10102	44.3	1	22.418	21.418
10102	44.7	1	22.489	22.731
10102	45.1	1	22.619	24.083
10102	45.6	1	22.790	25.615
10102	45.9	1	22.655	26.654
10110	254.1	1	21.624	26.725
10110	254.2	1	21.626	26.455
10110	255.2	1	21.589	24.163
10110	256.0	1	21.481	21.864
10110	257.1	1	21.333	19.888
10110	258.6	1	21.242	16.831
10110	259.3	1	21.414	15.398
10110	259.7	1	21.305	14.495
10110	261.0	1	21.399	11.103
10110	261.7	1	21.309	9.225
10110	262.7	1	21.038	7.455
10111	262.8	1	21.564	11.824
10111	263.5	1	21.833	9.993
10111	264.4	1	21.499	8.198
10111	265.9	1	21.915	6.302
10111	266.5	1	22.031	4.988
10111	267.3	1	22.237	2.702
10111	267.4	1	22.241	2.418
10120	243.1	1	20.901	2.501
10120	243.3	1	20.868	2.855
10120	244.8	1	20.897	5.211
10120	245.5	1	20.901	6.330
10120	246.2	1	20.814	7.239
10120	247.2	1	21.381	9.171
10120	247.9	1	21.474	11.351
10120	249.2	1	21.458	14.459
10120	249.6	1	21.328	15.356
10120	250.1	1	21.090	16.646

LINE NO.	FIDUCIAL	MAP	POSITION (INCHES) X	Y
10120	251.2	1	21.043	19.114
10120	252.2	1	20.934	21.830
10120	252.9	1	20.897	24.213
10120	253.8	1	20.851	26.720
10120	253.9	1	20.839	26.978
10130	231.2	1	20.249	26.174
10130	231.9	1	20.194	24.172
10130	233.2	1	20.174	21.920
10130	234.5	1	20.094	19.071
10130	235.4	1	19.929	17.011
10130	236.7	1	19.778	13.999
10130	237.6	1	19.510	11.671
10130	238.2	1	19.095	9.832
10130	239.3	1	18.549	7.463
10130	240.4	1	18.923	5.362
10130	241.9	1	19.862	2.564
10136	36.8	1	20.070	11.549
10136	37.4	1	20.159	10.228
10136	38.1	1	20.274	8.503
10136	38.8	1	19.995	7.377
10136	39.4	1	20.093	6.469
10136	40.4	1	20.208	5.043
10136	41.2	1	20.122	3.517
10136	41.6	1	20.084	2.505
10140	220.3	1	18.633	2.585
10140	220.4	1	18.663	2.879
10140	221.9	1	18.930	5.366
10140	223.2	1	18.864	6.853
10140	224.5	1	19.065	9.638
10140	225.3	1	19.114	11.887
10140	225.7	1	19.197	12.837
10140	226.3	1	19.323	14.006
10140	228.2	1	19.495	17.903
10140	228.8	1	19.554	19.067
10140	229.8	1	19.528	21.992
10140	230.4	1	19.454	24.081
10140	231.1	1	19.280	26.349
10150	208.6	1	18.273	26.379
10150	208.9	1	18.600	25.160
10150	209.6	1	18.635	23.402
10150	210.9	1	18.650	21.080
10150	211.8	1	18.622	20.046
10151	212.0	1	18.010	20.879
10151	212.8	1	18.102	18.354
10151	213.4	1	18.366	16.742
10151	214.6	1	18.430	14.665
10151	215.3	1	18.403	13.155
10151	216.0	1	18.276	11.546

LINE NO.	FIDUCIAL	MAP	POSITION (INCHES) X	Y
10151	216.8	1	18.150	9.648
10151	218.1	1	17.810	6.935
10151	219.6	1	17.890	2.896
10160	198.0	1	17.823	3.061
10160	199.7	1	17.680	5.918
10160	200.6	1	17.710	7.221
10160	202.1	1	17.979	10.110
10160	202.7	1	17.957	11.631
10160	203.7	1	18.067	13.581
10160	204.2	1	18.063	14.601
10160	205.2	1	18.166	16.863
10160	205.8	1	18.076	18.352
10160	206.7	1	17.973	20.557
10160	207.8	1	17.751	23.487
10160	208.3	1	17.681	25.193
10160	208.5	1	17.608	25.758
10170	187.6	1	16.962	25.243
10170	188.0	1	16.871	24.068
10170	189.0	1	17.049	21.908
10170	190.3	1	17.190	20.634
10170	191.4	1	17.394	18.903
10170	192.0	1	17.264	17.227
10170	193.1	1	17.035	14.788
10170	194.2	1	16.565	11.937
10170	195.1	1	16.248	9.382
10170	196.1	1	15.806	6.698
10170	197.2	1	16.653	2.892
10175	29.1	1	16.891	14.509
10175	30.5	1	16.865	11.053
10175	31.2	1	16.800	9.304
10175	32.8	1	16.989	5.509
10175	33.7	1	17.179	3.076
10182	177.5	1	16.506	2.816
10182	179.6	1	15.683	6.790
10182	181.2	1	16.140	9.721
10182	182.0	1	16.314	11.661
10182	183.0	1	16.369	13.965
10182	183.9	1	16.262	16.366
10182	184.9	1	15.937	18.755
10182	185.7	1	16.058	20.624
10182	186.7	1	15.954	23.122
10182	187.5	1	15.962	25.408
10190	154.9	1	15.726	25.919
10190	155.6	1	15.382	23.488
10190	156.9	1	15.430	20.995
10190	158.7	1	15.447	17.622
10190	159.5	1	15.316	16.115
10190	160.1	1	15.233	14.801

LINE NO.	FIDUCIAL	MAP	POSITION (INCHES) X	Y
10190	161.2	1	15.076	12.418
10190	161.9	1	14.870	10.869
10190	163.0	1	14.431	8.453
10190	163.6	1	14.256	7.035
10190	164.4	1	14.198	4.737
10191	165.6	1	15.711	17.214
10191	166.0	1	15.550	16.219
10191	166.6	1	15.627	14.708
10191	167.6	1	15.557	12.239
10191	170.6	1	15.043	6.241
10191	172.0	1	16.264	2.852
10200	143.4	1	14.582	2.744
10200	144.2	1	14.954	4.375
10200	145.7	1	14.528	6.521
10200	146.9	1	14.447	8.452
10200	147.5	1	14.450	9.937
10200	149.1	1	14.745	13.364
10200	149.4	1	15.038	13.835
10200	149.8	1	15.409	14.643
10200	150.3	1	15.343	15.654
10200	150.6	1	15.307	16.195
10200	151.5	1	15.179	18.065
10200	153.0	1	14.878	20.756
10200	154.1	1	14.470	23.819
10200	154.5	1	14.425	24.892
10200	154.8	1	14.334	25.633
10205	21.5	1	15.205	9.849
10205	22.1	1	15.186	11.217
10205	22.6	1	15.204	12.442
10205	23.2	1	15.196	13.982
10205	23.9	1	15.094	15.467
10205	26.4	1	14.657	21.179
10205	27.3	1	14.631	23.378
10205	27.9	1	14.435	25.124
10210	131.7	1	14.070	25.930
10210	132.8	1	13.883	23.134
10210	134.6	1	13.765	20.946
10210	136.0	1	13.709	19.092
10210	137.8	1	13.703	15.340
10210	138.5	1	13.815	13.842
10210	139.3	1	13.857	12.083
10210	140.1	1	13.729	10.711
10210	140.7	1	13.563	9.246
10210	141.7	1	13.283	6.183
10210	142.3	1	13.621	4.339
10210	142.7	1	13.571	2.909
10221	120.0	1	13.109	2.978
10221	121.7	1	12.989	6.079

LINE NO.	FIDUCIAL	MAP	POSITION (INCHES) X	Y
10221	123.2	1	13.062	9.170
10221	124.6	1	13.288	11.319
10221	125.6	1	13.282	13.306
10221	126.4	1	13.451	15.188
10221	127.1	1	13.422	16.507
10221	128.6	1	13.281	19.626
10221	129.2	1	13.242	20.876
10221	130.3	1	13.139	22.620
10221	130.9	1	12.989	24.068
10221	131.6	1	12.925	26.027
10230	100.5	1	12.143	25.899
10230	101.5	1	12.070	23.125
10230	102.7	1	12.095	21.036
10231	103.5	1	11.960	21.934
10231	103.9	1	11.909	20.763
10231	104.4	1	12.094	19.362
10231	105.6	1	12.155	16.487
10231	106.2	1	12.322	15.539
10231	107.0	1	12.062	13.900
10231	107.5	1	12.001	12.981
10231	109.0	1	11.653	10.820
10231	109.9	1	11.438	9.198
10231	110.9	1	11.761	6.415
10231	112.0	1	11.884	3.358
10235	15.4	1	12.293	16.353
10235	15.9	1	12.250	15.252
10235	16.4	1	12.107	14.103
10235	17.1	1	12.016	12.674
10235	17.8	1	12.132	11.457
10235	18.4	1	12.105	10.428
10235	19.0	1	12.086	8.824
10235	19.9	1	11.866	6.364
10235	21.1	1	11.510	3.289
10240	87.8	1	11.239	3.260
10240	88.4	1	11.453	4.151
10240	89.5	1	11.408	6.094
10240	90.5	1	11.414	8.002
10240	91.6	1	11.340	9.793
10240	93.4	1	11.322	12.504
10240	94.7	1	11.239	14.517
10240	95.8	1	11.070	16.319
10240	97.6	1	11.393	19.160
10240	98.6	1	11.446	20.884
10240	99.2	1	11.507	22.666
10240	99.7	1	11.410	24.154
10240	100.3	1	11.384	25.690
10250	76.5	1	10.694	25.193
10250	76.8	1	10.520	24.243

LINE NO.	FIDUCIAL	MAP	POSITION (INCHES) X	Y
10250	77.5	1	10.415	22.354
10251	78.4	1	10.607	22.338
10251	79.9	1	10.534	18.804
10252	80.4	1	9.988	18.885
10252	80.9	1	10.504	17.372
10252	82.2	1	10.353	15.226
10252	83.1	1	10.043	13.578
10252	83.9	1	10.050	12.211
10252	84.9	1	10.246	9.927
10252	86.0	1	10.338	6.454
10252	87.0	1	10.646	4.113
10252	87.3	1	10.793	3.102
10260	63.5	1	10.205	2.767
10260	64.0	1	10.060	3.891
10260	65.1	1	9.638	5.143
10260	66.4	1	9.679	7.367
10260	68.9	1	9.454	11.922
10260	70.4	1	9.473	14.821
10260	71.5	1	9.479	16.746
10260	72.2	1	9.513	17.944
10260	75.2	1	9.675	22.942
10260	75.7	1	9.851	24.050
10260	76.4	1	9.787	25.763
10270	52.4	1	9.234	25.664
10270	53.2	1	8.995	23.374
10270	53.6	1	8.897	22.069
10271	54.6	1	9.343	21.950
10271	56.3	1	9.027	17.630
10271	57.5	1	9.144	15.269
10271	59.4	1	9.271	11.613
10271	60.6	1	8.990	9.317
10271	61.6	1	9.127	7.067
10271	62.3	1	9.153	5.184
10271	62.9	1	9.350	3.388
10271	63.1	1	9.354	2.710
10280	40.1	1	8.726	3.211
10280	40.3	1	8.770	3.582
10280	41.7	1	8.661	5.352
10280	42.6	1	8.481	6.555
10280	43.7	1	8.542	9.300
10280	45.0	1	8.382	11.096
10280	46.7	1	8.402	14.309
10280	48.6	1	8.163	17.418
10280	49.7	1	8.194	19.459
10280	51.2	1	8.323	22.330
10280	52.0	1	8.210	24.551
10280	52.3	1	8.258	25.607
10290	28.7	1	7.529	26.594

LINE NO.	FIDUCIAL	MAP	POSITION (INCHES) X	Y
10290	29.0	1	7.494	25.635
10290	29.8	1	7.502	23.136
10290	30.9	1	7.505	20.793
10291	31.0	1	7.829	22.299
10291	31.6	1	7.490	20.383
10291	32.1	1	7.586	19.062
10291	32.8	1	7.764	17.731
10292	33.0	1	7.753	17.802
10292	33.5	1	7.525	16.819
10292	34.9	1	7.519	14.419
10292	36.7	1	7.480	11.298
10292	37.5	1	7.537	9.165
10292	38.3	1	7.638	6.758
10292	39.6	1	7.734	3.083
10305	12.4	1	7.340	3.235
10305	13.6	1	6.899	6.601
10305	14.4	1	6.930	9.074
10305	15.8	1	6.879	11.822
10305	16.8	1	6.606	13.948
10305	18.4	1	6.458	17.383
10305	19.6	1	6.380	20.254
10305	21.4	1	6.491	24.151
10305	21.8	1	6.594	25.476
10310	87.0	1	5.774	25.900
10310	87.4	1	5.810	24.944
10310	87.8	1	5.798	23.672
10310	88.9	1	5.683	20.716
10311	89.3	1	5.426	21.471
10311	89.7	1	5.413	19.818
10311	91.9	1	5.955	14.684
10311	92.7	1	6.121	12.678
10311	93.1	1	6.116	11.572
10311	94.9	1	6.095	8.615
10311	96.5	1	5.822	4.486
10320	61.5	1	4.998	4.385
10320	61.6	1	5.006	4.602
10320	64.3	1	5.654	10.245
10320	65.4	1	5.491	11.583
10320	65.9	1	5.846	12.699
10320	66.9	1	5.950	14.681
10320	68.0	1	6.079	17.411
10320	69.1	1	5.631	20.218
10322	80.1	1	5.055	10.099
10322	80.7	1	5.234	11.588
10322	81.1	1	5.341	13.010
10322	82.3	1	5.295	15.006
10322	83.2	1	5.126	17.610
10322	84.1	1	5.082	19.802

LINE NO.	FIDUCIAL	MAP	POSITION (INCHES) X	Y
10322	85.4	1	5.077	22.116
10322	86.6	1	4.834	25.515
10322	86.9	1	4.825	26.150
10330	49.9	1	4.537	25.868
10330	50.2	1	4.322	24.973
10330	51.3	1	4.051	21.778
10331	51.8	1	4.342	21.764
10331	52.6	1	4.046	19.242
10331	53.5	1	4.266	17.556
10331	55.4	1	4.715	14.224
10331	56.0	1	4.835	12.890
10331	56.6	1	4.927	11.581
10331	58.4	1	4.583	9.163
10331	59.7	1	4.162	5.584
10331	60.0	1	3.992	4.706
10340	40.8	1	3.731	5.138
10340	42.0	1	3.894	7.412
10340	42.6	1	3.863	8.692
10340	43.2	1	3.878	10.498
10340	43.8	1	3.771	11.612
10340	44.4	1	3.269	13.184
10340	45.7	1	3.258	14.752
10340	47.3	1	3.282	19.011
10340	48.8	1	3.542	22.692
10340	49.4	1	3.443	24.459
10340	49.8	1	3.354	25.440
10350	30.9	1	2.434	25.988
10350	31.3	1	2.594	24.978
10350	31.8	1	2.596	23.377
10350	32.3	1	2.661	21.613
10350	33.1	1	2.538	19.709
10351	33.4	1	2.313	21.333
10351	33.8	1	2.284	19.705
10351	34.8	1	2.795	16.970
10351	35.8	1	3.162	14.716
10351	36.5	1	3.430	13.087
10351	37.2	1	3.526	11.718
10351	37.6	1	3.595	10.572
10351	38.7	1	3.138	7.656
10351	39.0	1	2.898	6.490
10351	39.5	1	2.621	5.161
10351	39.6	1	2.555	4.901
10360	23.7	1	2.400	5.068
10360	24.7	1	1.943	7.287
10360	26.0	1	1.587	11.580
10360	26.5	1	1.433	12.914
10360	27.7	1	0.975	15.521
10360	28.1	1	0.881	16.270

LINE NO.	FIDUCIAL	MAP	POSITION (INCHES) X	Y
10360	28.7	1	0.794	17.933
10360	29.3	1	1.278	20.006
10360	29.8	1	1.398	21.838
10360	30.2	1	1.602	23.557
10360	30.5	1	1.769	24.330
10365	7.8	1	1.934	5.066
10365	8.4	1	1.883	6.318
10365	8.8	1	1.938	7.329
10365	10.1	1	2.257	10.923
10365	10.6	1	2.210	12.403
10365	11.9	1	2.021	14.905
10365	12.9	1	2.007	17.473
10365	13.6	1	2.037	19.551
10365	14.2	1	1.898	21.315
10365	14.8	1	1.776	23.602
10365	15.2	1	1.528	24.591
10370	15.3	1	1.153	24.539
10370	16.4	1	0.902	21.591
10370	17.2	1	0.866	19.697
10371	17.9	1	0.576	19.467
10371	18.3	1	0.795	18.051
10371	18.8	1	0.941	16.828
10371	19.3	1	1.182	15.764
10371	20.1	1	1.531	13.703
10371	20.8	1	1.475	11.590
10371	21.5	1	1.551	9.205
10371	22.4	1	1.385	6.608
10371	22.9	1	1.407	5.362
10371	23.0	1	1.375	5.035
10380	9.6	1	-0.217	9.651
10380	9.8	1	-0.008	10.280
10380	10.1	1	0.190	11.411
10380	10.6	1	0.341	13.003
10380	11.4	1	0.229	14.924
10380	12.3	1	-0.092	16.412
10380	13.0	1	-0.034	17.653
10380	14.1	1	-0.138	21.136
10380	14.9	1	-0.010	23.902

APPENDIX A

BARRINGER/QUESTOR MARK VI INPUT(R) Helicopter System

The INduced PUlse Transient (INPUT) method is a system whereby measurements are made, in the time domain, of a secondary electromagnetic field while the primary field is between pulses. Currents are induced into the ground by means of a pulsed primary electromagnetic field which is generated from a transmitting loop around the helicopter. By using half-sine wave current pulses (Figure A-1) and a transmitter loop of large turns-area, a high signal-to-noise ratio and the high output power needed for deep penetration, are achieved.

Induced current in a conductor produces a secondary electromagnetic field which is detected and measured after the termination of each primary pulse. Detection of the secondary field is accomplished by means of a receiving coil, wound on an air core form, mounted in a PCV plastic shell called a "bird" and towed behind and below the helicopter on 76 metres (250 feet) of coaxial cable. The received signal is processed and recorded by equipment within the helicopter.

The axis of the receiving coil may be vertical or horizontal relative to the flight direction. In rolling or hilly terrain the standard or horizontal coil axis is preferred, although in steep terrain, the vertical axis coil optimizes coupling with horizontal or dipping stratigraphy. The secondary field is in the form of a decaying voltage transient, measured in time, at the termination of the primary transmitted pulse. The amplitude of the transient is proportional to the amount of

measured in time, at the termination of the primary transmitted pulse. The amplitude of the transient is proportional to the amount of current induced into the conductor, the conductor dimensions, conductivity and the depth beneath the aircraft.

The rate of decay of the transient is inversely proportional to conductance. By sampling the decay curve at six different time intervals and recording the amplitude of each sample, an estimate of the relative conductance can be obtained. Transients due to strong conductors such as sulphides and graphite, usually exhibit long decay curves and are therefore commonly recorded on all six channels. Sheet-like surface conductive materials, on the other hand, have short decay curves and will normally only show a response in the first two or three channels.

For homogeneous conditions, the transient decay will be exponential and the time constant of decay is equal to the time difference at two successive sampling points divided by the log ratio of the amplitudes at this point.

TRANSMITTER SPECIFICATIONS

Pulse Repetition Rate	180	per sec
Pulse	Half sine	
Pulse Width	2.0	millisec
Off Time	3.56	millisec
Output Voltage	67	volts
Output Current Peak	200	amperes
Output Current Average	46	amperes
Coil Area	177 $m.^2$	(1,904 $ft.^2$)
Coil Turns	7	
Electromagnetic Field Strength (peak)	247,800	amp-turn-$meter^2$

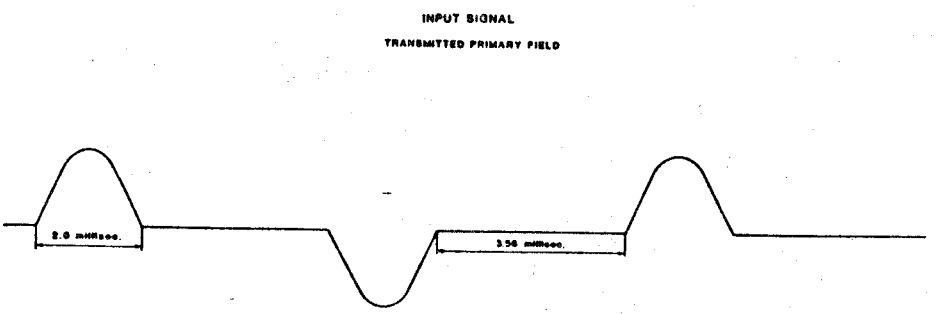

Figure A1

RECEIVER SPECIFICATIONS

Sample Gate	Windows (centre positions)	Widths
CH 1	340 sec	200 sec
CH 2	540	200
CH 3	840	400
CH 4	1240	400
CH 5	1740	600
CH 6	2340	600

Sample Interval	0.5 sec
Integration Time Constant	1.3 sec
Bird Position behind Aircraft (at 40 kt)	19 metres
Bird Position below Aircraft (at 40 kt)	73 metres

Receiver features: Power Monitor 50 or 60 Hz

50 or 60 Hz and Harmonic Filter

VLF Rejection

Spheric Rejection (tweak) Filter

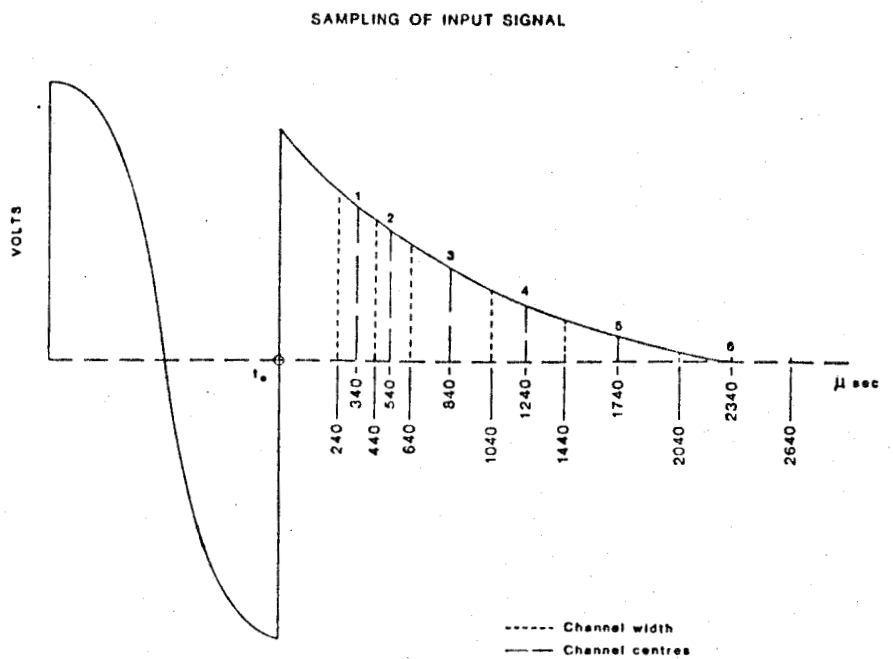

Figure A2

DATA ACQUISITION SYSTEM

Sonotek SDS 1200

9 track 800 BPI ASCII

Includes time base Intervalometer, Fiducial System

CAMERA

Geocam 75 SF

35 mm continuous strip or frame

TAPE DRIVE

Digidata Model 1139

OSCILLOSCOPE

Tektronix Model 305

ANALOG RECORDER

Honeywell Visicorder WS 4010

Kodak Light Sensitive Pape (15cm)

Recording 14 Channels: 50-60 Hz Monitor, 6 INPUT Channels, fine and coarse Magnetics, Altimeter, vertical and horizontal timing lines and fiducial markers.

ALTIMETER

Sperry Radar Altimeter

SONOTEK P.M.H. 5010 PROTON MAGNETOMETER

The airborne magnetometer is a proton free precession sensor, which operates on the principle of nuclear magnetic resonance to produce a measurement of the total magnetic intensitity. It has a sensitivity of 1 gamma and an operating range of 20,000 gammas to 100,000 gammas. The sensor is a solenoid type, oriented to optimize results in a low ambient magnetic field. The sensor housing is mounted on the tip of the nose boom supporting the INPUT transmitter cable loop. A 3-term compensating coil and perma-alloy strips are adjusted to counteract the effects of permanent and induced magnetic fields in the aircraft.

Because of the high intensity electromagnetic field produced by the INPUT transmitter, the magnetometer and INPUT results are sampled on a time-share basis. The magnetometer head is energized while the transmitter is on, but a measurement is only obtained during a short period when the transmitter is off. Using this technique, the sensor head is energized for 0.80 seconds and subsequently the precession frequency is recorded and converted to gammas during the following 0.20 seconds when no current pulses are induced into the transmitter coil.

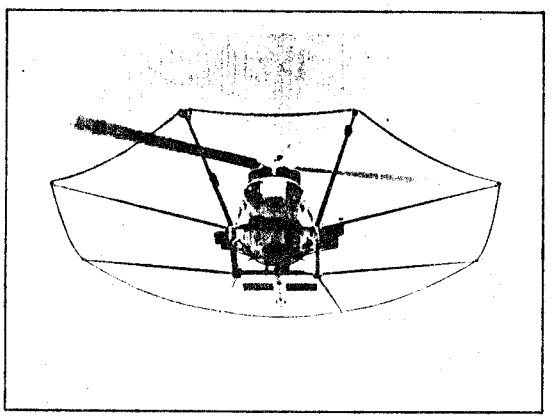

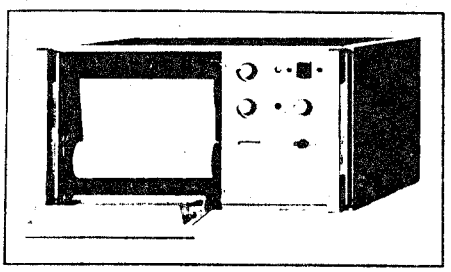

HONEYWELL ANALOGUE CHART RECORDER

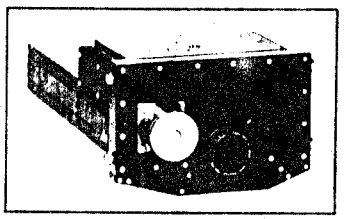

35mm TRACKING CAMERA

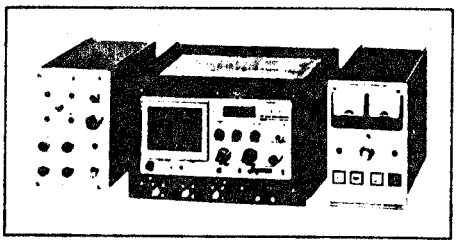

INTERFACE, OSCILLOSCOPE & T.C.U.

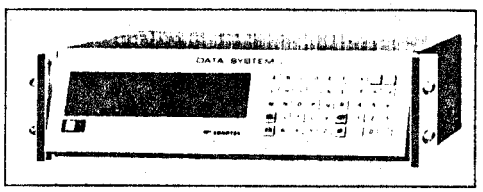

SONOTEK DATA SYSTEM

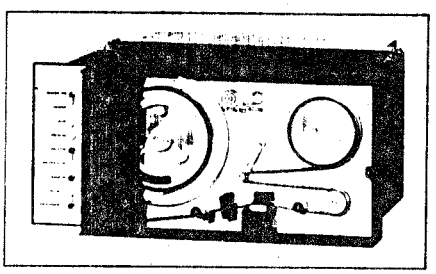

9 TRACK TAPE RECORDER

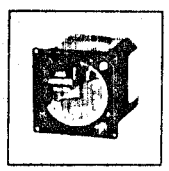

RADAR ALTIMETER

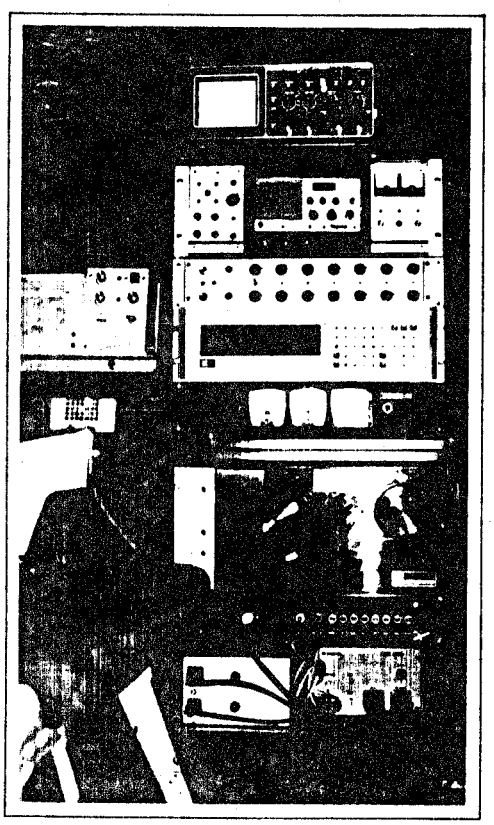

INPUT® EQUIPMENT INSTALLATION

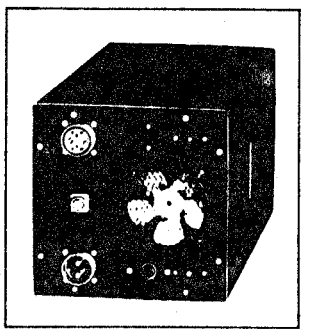

TRANSMITTER

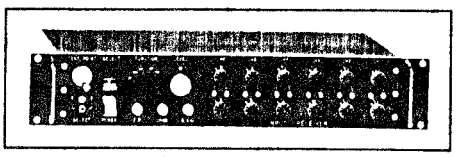

MK VI INPUT® RECEIVER

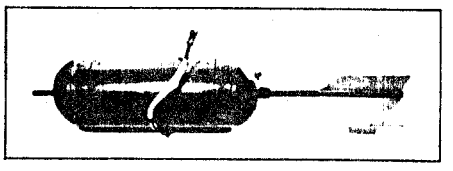

TOWED "BIRD" ASSEMBLY

QUESTOR/BARRINGER MARK VI "INPUT"® SYSTEM EQUIPMENT

APPENDIX B

The Survey Helicopter

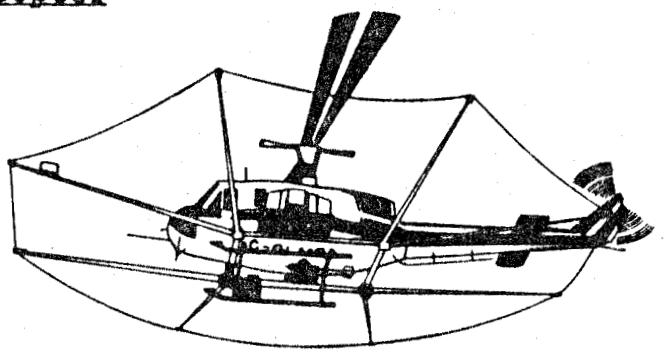

Figure B1

Manufacturer	Bell Helicopter Company
Type	205A-1
Canadian Registration	C-GLMC - present installation
Date of INPUT Installation	May 1982

Modifications:

1) Cradle and wing booms for transmitter coil mounting
2) Camera and altimeter mounting
3) Modified gasoline driven generator system

Any BELL 205-212 airframe can support the QUESTOR Helicopter INPUT system. The 205 is powered by one low maintenance turbine engine. The configuration of the helicopter provides for easy installation of equipment, which can be dissasembled and crated to the survey base. Reassembly takes less than two days. These factors have proven the helicopter to be a reliable and efficient geophysical survey system in areas not suitable for fixed-wing operation.

APPENDIX C

INPUT System Characteristics

a) Geometry

The INPUT system, a time domain airborne electromagnetic system, has the transmitter loop located around the helicopter airframe while the receiver, referred to as the 'bird', typically is towed 19 metres behind and 73 metres below the helicopter at a survey airspeed of 40 knots. The actual spatial position of the bird is dependent on the airspeed of the survey helicopter, as can be seen in Figure C1.

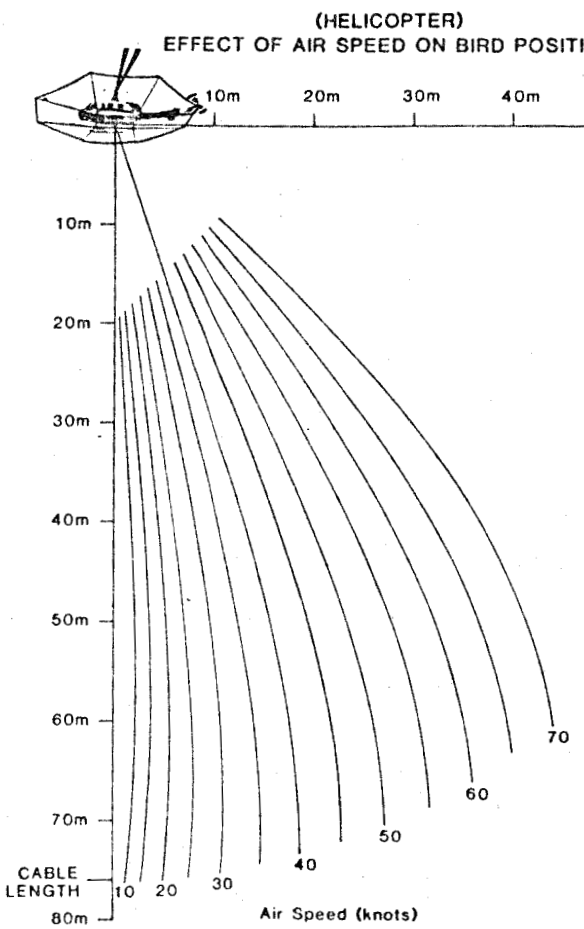

Figure C1

b) The Lag Factor

The bird's spatial position along with the time constant of the system introduces a lag factor (Figure C2) or shift of the response past the actual conductor axis in the direction of the flight line. This is due to fiducial markers being generated and imprinted on the film in real time and then merged with E.M. data which has been delayed due to the two aforementioned parameters. This lag factor necessitates that the receiver response be normalized back to the helicopter's position for the map compilation process. The lag factor can be calculated by considering it in terms of time, plus the elapsed distance of the proposed shift and is given by:us the elapsed distance of the proposed shift and is given by:

$$\text{Lag (seconds)} = \text{time constant} + \frac{\text{bird lag (metres)}}{\text{ground speed (metres/sec)}}$$

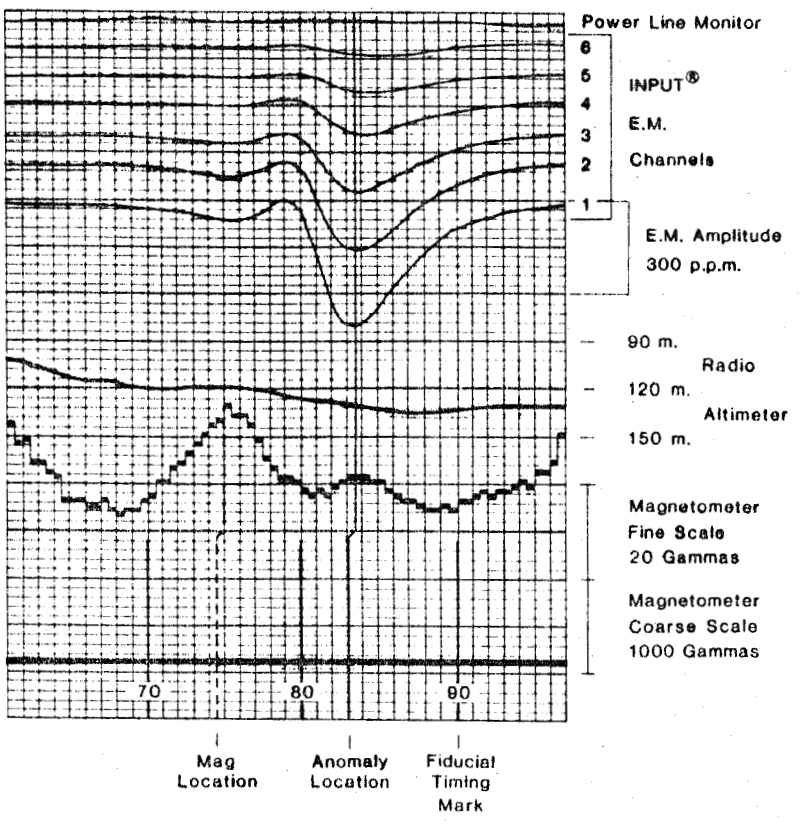

Figure C2

The time constant introduces a 1.3 second lag while, at an aircraft velocity of 40 kt., the 'bird' lag is 1 second. The total lag factor which is to be applied to the INPUT E.M. data at 40 kts. is 2.3 seconds. It must be noted that these two parameters vary within a small range dependent on the helicopter velocity, though they are applied as constants for consistency. As such, the removal of this lag factor will not necessarily position the anomalies in a straight line over the real conductor axis. The offset of a conductor response peak is a function or the system and conductor geometry as well as conductivity.

The magnetic data has a 1.0 second lag factor introduced relative to the real time fiducial positions. This factor is software controlled with the magnetic value recorded relative to the leading edge (left end) of each step 'bar', for both the fine and coarse scales. For example, a magnetic value positioned at fiducial 10.00 on the records would be shifted to fiducial 9.95 along the flight path.

A lag factor of 2 seconds (0.1 fiducial) is introduced to correct 50-60 Hz monitor for the effects of bird position and signal processing. In cases where a 50-60 Hz signal is induced in along formational conductor, a 50-60 Hz secondary electromagnetic transient may be detected as much as 5 km. from the direct source over the conductive horizon.

The altimeter data has no lag introduced as it is recorded in real time relative to the fiducial markings.

c) Calibration

The major advance made during the transition from the INPUT MK V to the INPUT MK VI has been the ability to calibrate the equipment accurately and consistently. Field tests at established test sites are carried out on an average of once every 6 months to check the consistency of the INPUT installations available from QUESTOR.

To calibrate the equipment for a survey operation the following tests are used:

1) "ZERO" the digital and record background E.M. levels;
2) magnetometer scale calibrations;
3) altimeter calibration;
4) calibration of INPUT receiver gain;
5) aircraft compensation;
6) record background E.M. levels at 600 m.;
7) survey flight;
8) record background E.M. levels at 600 m.
9) record full scale INPUT receiver gain;
10) record compensation drift;
11) terminate or repeat from step 4.

This sequence of tests may be repeated in midflight given that the duration of the flight is sufficiently long. Typically, this process is conducted every 2 hours of actual flying time and at the termination of every flight.

The background levels are recorded and then used to determine the drift that may occur in the E.M. channels during the progression of a survey flight. If drift has occurred, the

E.M. channels are brought back to a levelled position by use of the linear interpolation technique during the data processing.

The primary electromagnetic field generated by the INPUT system induces eddy currents in the frame of the helicopter. This spurious secondary field is a significant source of noise which needs to be taken account of before every survey flight is initiated.

Compensation is the technique by which the effects of this spurious secondary field are eliminated. A reference signal, which is equal in amplitude and waveform but opposite in polarity, is obtained from the primary field voltage in the receiver coil and applied to each channel of the receiver. The compensation signal is not a constant value due to coupling differences induced by 'bird' motion relative to the aircraft. The signal applied is proportional to the inverse cube of the distance between the 'bird' and aircraft. Figure C3 displays the effect of compensation.

Typically, channel 5 is selected for compensation because it is not affected by geological noise due to its sampling location in the transient and then coupling changes are induced by precipitating 'bird' motion. Phase considerations of channel 5, relative to the remaining channels, dictates whether sufficient compensation has been applied. If the remaining channels are in-phase to channel 5 during this procedure, an over-compensated situation is indicated, whereas, out-of-phase would be indicative of an under-compensation case. Normally this adjustment is carried out at an altitude of 600 metres in

order to eliminate the influence of external geological and cultural conductors.

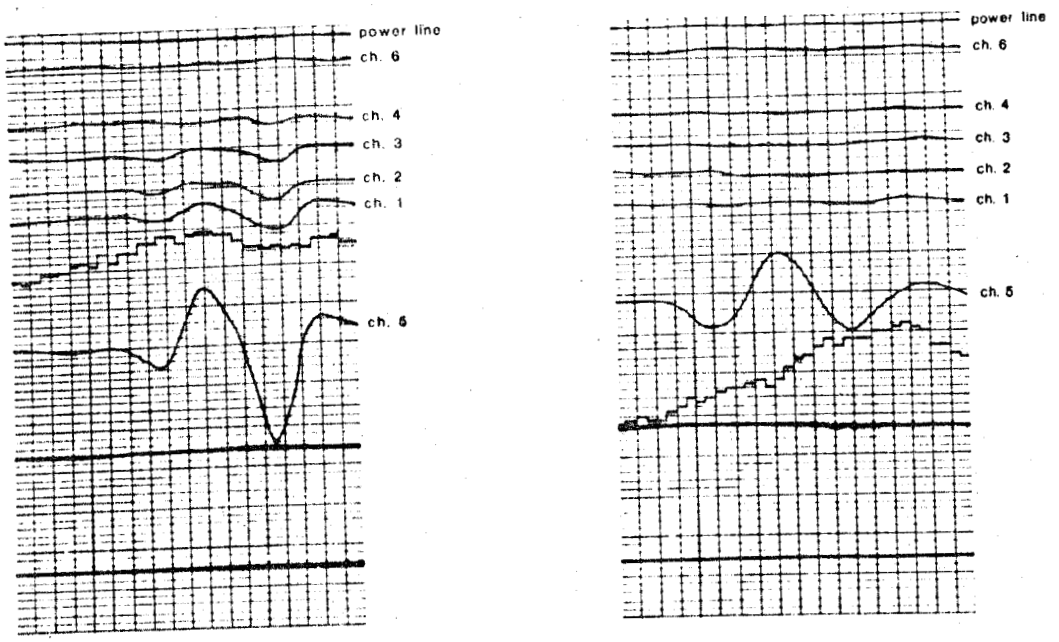

Uncompensated Compensated

Figure C3

The magnetometer, altimeter and INPUT receiver gain are also calibrated at the initiation of every survey flight. With the magnetometer, there are two scales, a coarse and a fine scale. The fine scale indicates a 10 gamma change for a 1 cm. change in amplitude (Figure C2). The coarse scale moves 2 mm. (or 1 division) for a 100 gamma change with full scale,2 cm., indicating a 1000 gamma shift.

The altimeter (Figure C4), is calibrated to indicate 400 feet altitude at the seventh major division (7 cm.), read from the bottom of the analog record. This is the nominal flying

height of INPUT surveys, wherever relief and aircraft performance are not limiting factors. The eighth major division correlates with 300 feet while the sixth corresponds with 500 feet in altitude.

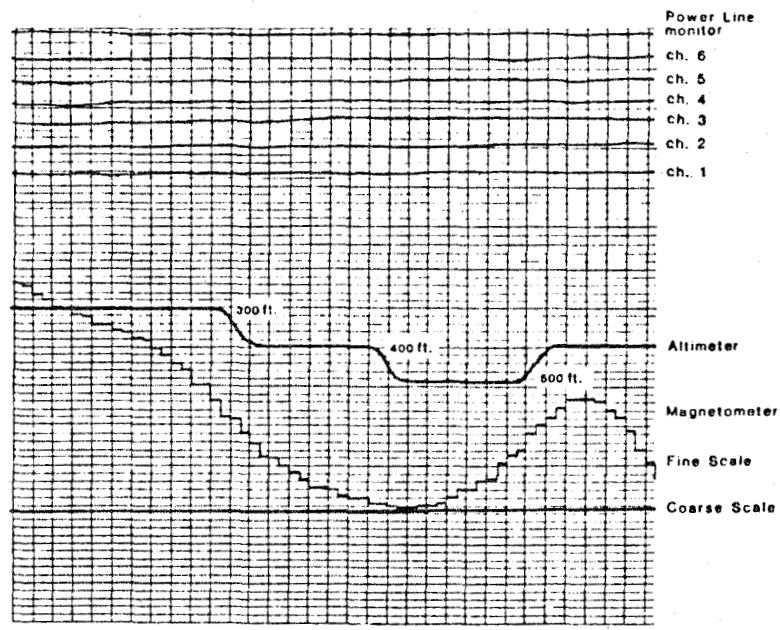

Figure C4

The INPUT receiver gain is expressed in parts per million of the primary field amplitude at the receiver coil. At the 'bird', the primary field strength is 8.5 and 8 volts peak-to-peak, for the vertical and horizontal axis coils respectively or 4.2 and 4.0 volts peak amplitude. The calibration signal introduced at the input stage of the receiver is 4.0 mV. Expressed in parts- per-million, this induces a change of:

$$\frac{4 \times 10\text{-}3 \times 10^{6}}{4.2} = 1{,}000 \text{ ppm (vertical coil)}$$

These calibration signals (Figure C5) cause an 8 cm. deflection of all 6 traces which translates to a sensitivity of 125 ppm/cm. for the vertical axis receiver coil system.

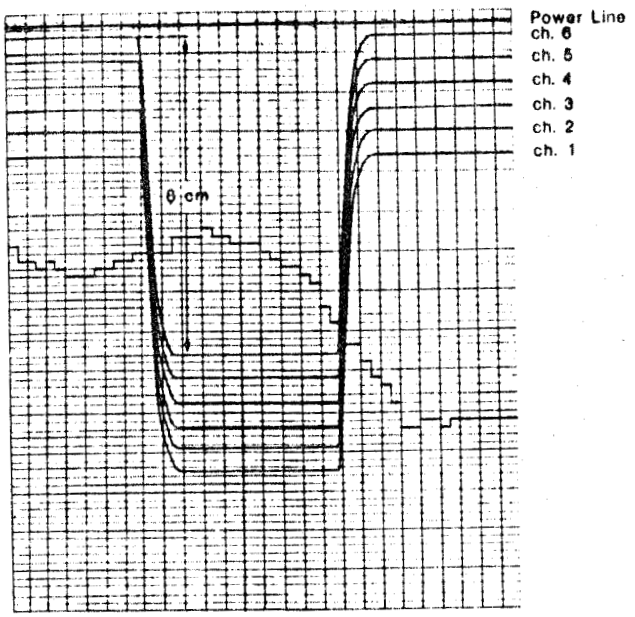

Figure C5

With the chart speed increased from the normal 0.25 cm. to 2.5 cm. per second, the time constant of the system (Figure C6), can be obtained by analysis of the exponential rise of the calibration signal for all 6 traces. The time constant, is defined as the time for the calibrated voltage to build up or decay to 63.2% of its final of initial value. A longer time constant reduces background noise but also has the effect of reducing the amplitude of the signal, especially for near surface responses.

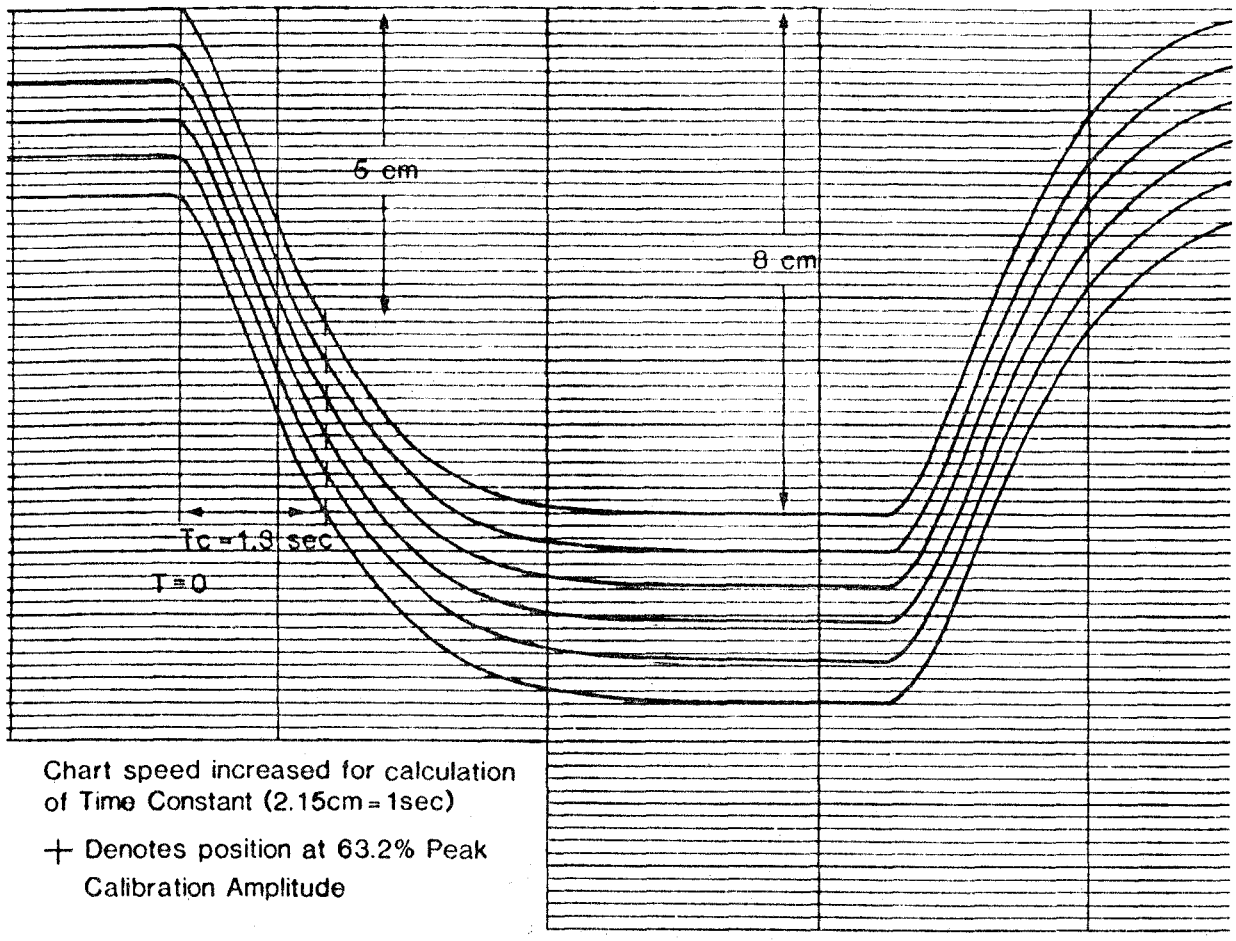

Figure C6

This trade-off indicates the importance of selecting an optimum value for the time constant. Experience and years of testing have indicated that a time constant of 1.3 second does not impede interpretation of bedrock source conductors.

d) Depth Penetration Capabilities

There are many factors which effect the depth of penetration. These factors consist of:

1) altitude of the helicopter above the ground;
2) conductivity contrast between conductor and host rock;
3) size and attitude of conductor;
4) type and conductivity of overburden present.

Of these factors, only the first parameter can be controlled. Typically, a survey altitude of 120 metres (400 feet) or less above the terrain is maintained. At this height, the helicopter INPUT MARK VI system has responded to conductors located at a depth of 200 metres (650 feet) below the surface.

APPENDIX D

INPUT Data Processing

The QUESTOR designed and implemented computer software routines for automatic interactive compilation and presentation, may be applied to all QUESTOR INPUT Systems. The software is compatible with the fixed-wing MARK VI INPUT, and the helicopter MARK VI INPUT. The procedures are all common, however, separate subroutines are accessed which contain the unique parameters to each system. Although many of the routines are standard data manipulations such as error detection, editing and levelling, several innovative routines are also optionally available for the reduction of INPUT data. The flow chart on the following page (Figure D1) illustrates some of the possibilities. Software and procedures are constantly under review to take advantage of new developments and to solve interpretational problems.

a) INPUT Data Entry and Verification

During the data entry stage, the digital data range is compared to the analog records and film. The raw data may be viewed on a high-resolution video graphics screen at any desirable scale. This technique is especially helpful in the identification of background level drift and instrument problems.

b) Levelling Electromagnetic Data

Instrument drift, recognized by viewing compressed data from several hours of survey flying, is corrected by an

interactive levelling program. Although only two or three calibration sequences are normally recorded, the QUESTOR technique permits the use of multiple non-anomalous background recordings to divide a possible problematic situation into segments. All 6 INPUT channels are levelled simultaneously, yet independently. The sensitivity of the levelling process is normally better than 10 ppm on data with a peak-to-peak noise level of 30 ppm.

c) Data Enhancement

Normal INPUT processing does not include the filtering of electromagnetic data. The residual high frequency variations often apparent on analog INPUT data, is due almost wholly to "spherics", atmospheric static discharges. In conductive environments, spherics are apparently grounded and effectively filtered. In resistive environments, frequency spectrum analysis and subsequent FFT (Fast Fourier Transform) filters have been applied to data to reduce the noise envelope.

d) Selection of EM Anomalies

The levelled data may be viewed sequentially on a graphics screen for the selection of INPUT anomalies. Anomalies are selected by aligning a cursor to the position of the peaks. Some of the parameters of the response are manually entered during the picking of the response. These include the number of channels above background levels and the type of anomaly, e.g. cultural, bedrock, surficial, up-dip, etc.

QUESTOR INPUT DATA PROCESSING

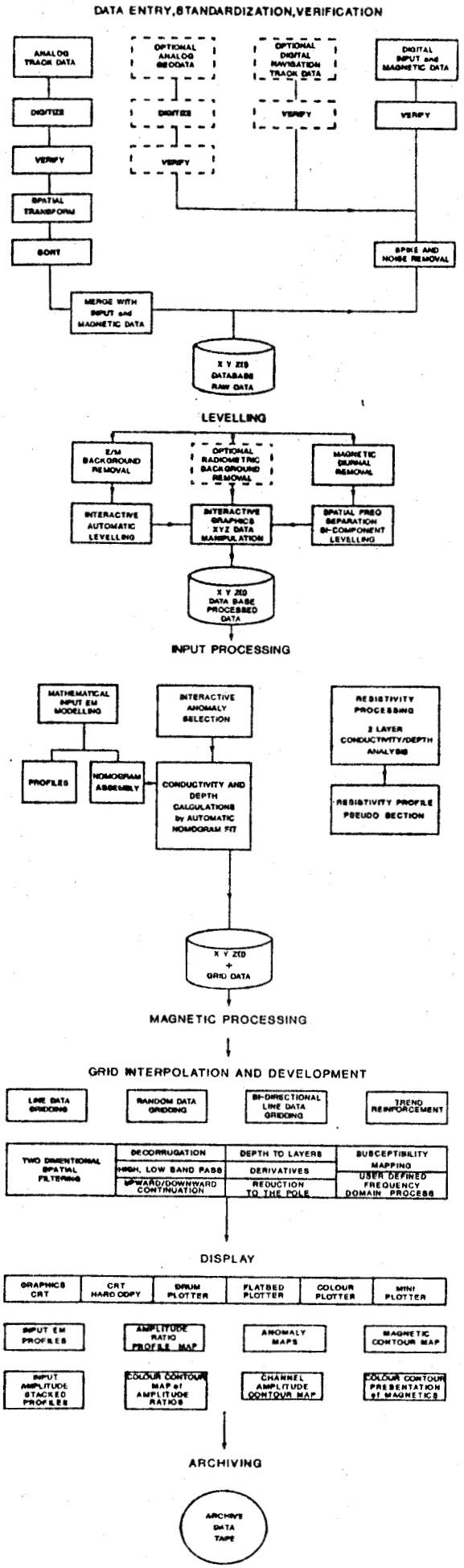

APPENDIX E

INPUT INTERPRETATION PROCEDURES

The INPUT system is dependent upon a definite resistivity contrast and is most suitable for highly conductive massive sulphides. Differentiation is possible between flat-lying surficial conductors and bedrock conductors.

The selection of anomalies is based on their characteristics and interpretation is sometimes enhanced by analyzing the magnetics. Spherics, due to atmospheric static discharges and lightning storms, are distinguishable from conductive anomalies. In the analysis of each conductor anomaly, the following parameters may be considered: anomaly shape with the conductor pattern, topography, corresponding magnetic features, anomaly decay rate, the number of channels affected, geological environment and strike direction and the interpreted dip relative to structural features.

For each anomaly selected, the following are recorded: location by fiducial, channel amplitudes in parts per million, number of channels, conductivity-thickness in siemens, corresponding magnetic association in gammas, magnetic fiducial location altitude of aircraft above ground in metres and also, the origin of the response (ie. surficial, bedrock, cultural).

Conductive responses are categorized into three main groups. These are bedrock, surficial and cultural.

Bedrock conductors can be sorted into conductive sources which are commonly encountered on INPUT surveys: massive

sulphides, graphites, serpentinized peridotites and fault or shear zones. Magnetite and manganese concentrations may also yield INPUT responses in some circumstances. INPUT responses over alkalic intrusives and weathered basic volcanics have been well documented by Macnae (1979) and Palacky (1979).

Massive Sulphides

Massive sulphides occur as both syngenetic and stratified deposits and as vein infilling deposits. Nickel deposits often occur as magmatic injections of massive sulphides. Kuroko-type syngenetic copper-zinc massive sulphides usually occur at an interface of felsic intermediate rocks. In this environment, there are seldom any significant formations of carbonaceous sediments on the same horizon. Often, these deposits are overlain by a silicious zone which may contain stingers of continuous sulphides, which change to disseminated sulphides away from the main deposit. These often give a deposit the appearance of a long strike-length zone which may not fit the explorationist's target model. A careful analysis of conductivities and apparent widths (half-peak-width), will often reveal the geometry and source. Syngenetic deposits of base metal sulphides of up to 2 km strike length are not unknown, although most sizeable deposits have strike lengths between 500 and 1000 m.

The conductivity of most massive sulphide deposits may be attributed to the pyrrhotite and chalcopyrite content, as both minerals form elongated interconnected masses which are most

amenable to the induction of electromagnetic secondary fields. Pyrite normally forms cubic crystals which must be interconnected electrically in order to produce a response. Massive pyrite often produces only a moderate response which may be difficult to distinguish from graphite. The in-situ conductivity of massive sulphides, although very high for individual crystals, often falls in the range of 5 to 20 S/m.

Sulphide conductive zones are rare in nature; economic sulphides are even more scarce. Long formational sulphide zones are known, but are not common. More often, sulphide concentrations may occur within formational graphitic zones.

The geometry of many syngenetic and injected sulphide deposits may fall within broad classifications of size, conductivity and magnetization but most of these bodies are anomalous within their local geological environment. There are often changes in dip, conductivity, thickness and magnetization with respect to the regional environment. There are no rules which apply universally to massive sulphide deposits. One observation which has consistently applied to sulphide deposits is that INPUT responses (amplitude and conductivity) are roughly proportional to mineral content.

The INPUT system is capable of detecting disseminated sulphides within zones of resistivity changes. These may have low conductivities and responses will normally be restricted to channels 1 through 4. The response amplitudes will vary with the horizontal and vertical extent of the zone. Gold deposits often fall within this response classification.

The magnetic response of a sulphide deposit is the most deceiving information available to the explorationist. Although many large economic deposits have a strong direct magnetic association, some of the largest base metal deposits have no magnetic association. An isolated magnetic anomaly caused by oxidation conditions at a volcanic vent flanking a conductor, may have more significance than a body which has a uniform magnetic anomaly along its strike length. Differing geochemical environments often results in the zoning of minerals so that non-homogeneous conductivities and magnetic responses may be favourable parameters.

Graphitic Carbonaceous Conductors

Carbonaceous sediments are usually found within the sedimentary facies of Precambrian and Proterozoic greenstone belts. These represent a low energy, sedimentary environment with good bedding planes and little or no structural deformation. Graphites are often located in basins of the sub-aqueous environment, producing the same body shape as sulphide concentrations. Most often however, they form long, homogeneous planar sequences. These may have thicknesses from a metre to hundreds of metres. The recognition of graphites in this setting is normally straightforward.

Conductivities and apparent widths may be very consistent along strike. Strike lengths of tens of kilometres are common for individual horizons.

The conductivity of a graphite unit is a function of two variables:

a) the quality and quantity of the graphite and

b) the presence of pyrrhotite as an accessory conductive mineral

Pyrite is the most common sulphide mineral which occurs within carbonaceous beds. It does not contribute significantly to the overall conductivity as it will normally be found as disseminated crystals. Greenschist facies metamorphosis will often be sufficient to convert carbonaceous sediments to graphitic beds. Likewise, pyrite will often be transformed to pyrrhotite.

Without pyrrhotite, most graphitic conductors have less than 20 S conductivity-thickness value as detected by the INPUT system or 1 to 10 S/m conductivity from ground geophysical measurements. With pyrrhotite content, there may be little difference from sulphide conductors.

It is not unusual to find local concentrations of sulphides within graphitic sediments. These may be recognized by local increases in apparent width, conductivity or as a conductor offset from the main linear trends.

Graphite has also been noted in fault and shear zones which may cross geological formations at oblique angles.

Serpentinized Peridotites

Serpentinized peridotites are very distinguishable from other anomalies. Their conductivity is low and is caused partially by magnetite. They have a fast decay rates, large amplitudes and strong magnetic correlation.

Magnetite

INPUT anomalies over massive magnetites correlate to the total Fe content. Below 25-30% Fe, little or no response is obtained. However, as the Fe percentage increses, strong anomalies result with a distinguished rate of decay that usually is more pronounced than those for massive sulphides.

Contact zones are often predicted when anomaly trends coincide with lines of maximum gradient along a flanking magnetic anomaly.

Surficial Conductors

Surficial conductors are characterized by fast decay rates and usually have a conductivity-thickness of 1-5 siemens. These values will be much higher in saline conditions. Overburden responses are broad, more so than bedrock conductors. Anomalies due to surficial conductivity are not dependent on flight direction. In profile form, surficial responses are symmetrical from line-to-line with the Helicopter INPUT system, and are characterized by a single response rather than a double peak for dipping and vertical conductors. Conductive deposits such as clay beds, may lie in valleys which can be checked on the altimeter trace and with the base maps topography.

Cultural Conductors

Cultural conductors are identifiable by examining the power line monitor and the film to locate railway tracks, power lines, buidings, fences or pipe lines. Power lines produce INPUT

anomalies of high conductivity that are similar to bedrock responses. The strength of cultural anomalies is dependent on the grounding of the source. INPUT anomalies usually lag the power line monitor by 1 second, which should be consistent from line-to-line. If this distance between the INPUT response and the power line monitor differs between lines, then there is the possibility of an additional conductor present. The amplitude and conductivity-thickness of anomalies should be relatively consistent from line-to-line.

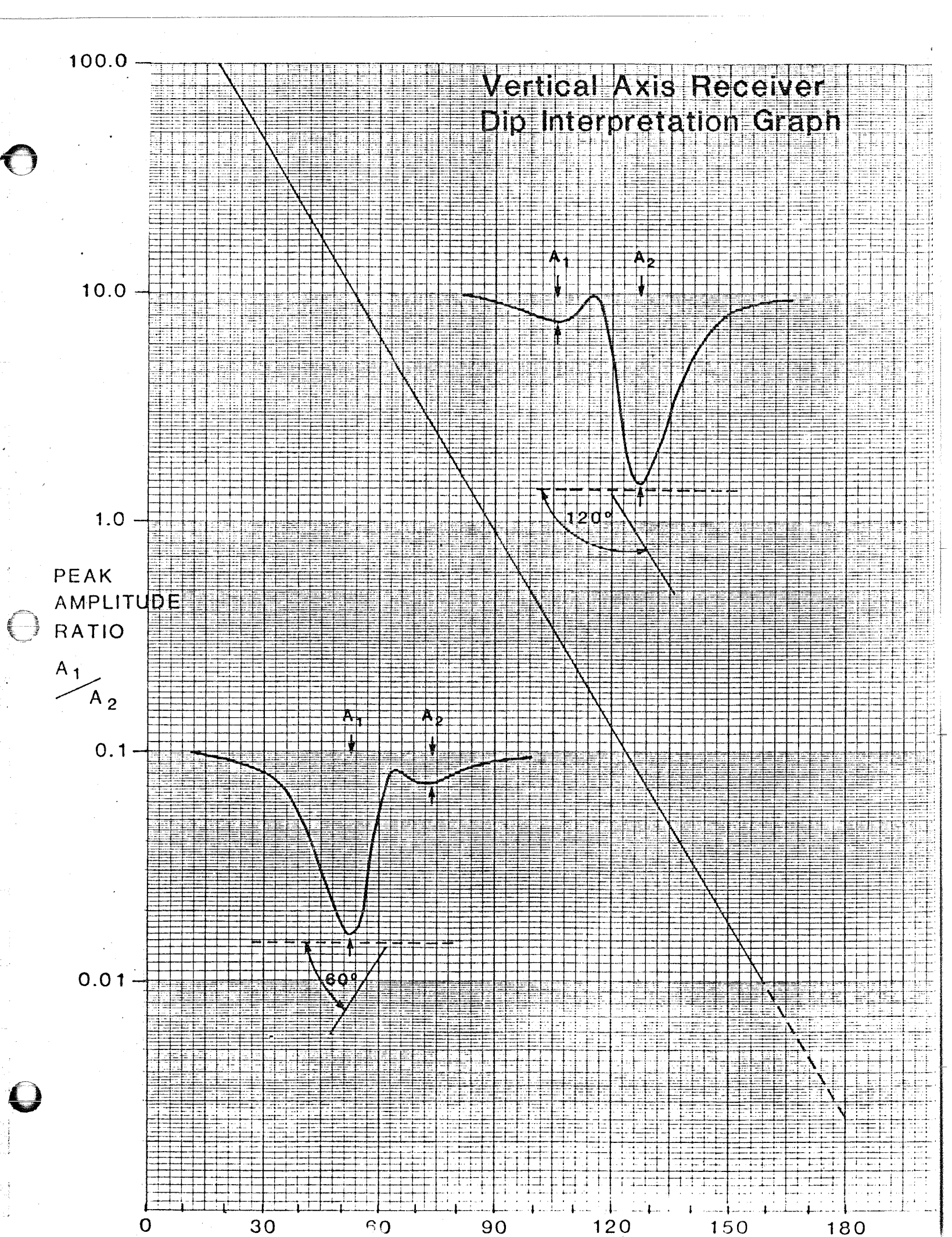
Vertical Axis Receiver
Dip Interpretation Graph
100.0
10.0
1.0
0.1
0.01
PEAK
AMPLITUDE
RATIO
A1/A2
A1
A2
120°
60°
0
30
60
90
120
150
180

APPENDIX F

INPUT Response Models

To the interpreter, one of the main advantages of the INPUT system geometry is the variation of the secondary response with conductor shape, size, depth and conductivity (Palacky 1976, 1977).

When we discuss the recognition parameters, one of the variables which is often omitted, is the plotting position of the main peaks in opposite flight directions on adjacent lines. In many cases, the responses may appear similar, but the plotting positions will show significant differences. These situations will be illustrated in the following section.

A third conductor identification factor is the INPUT decay transient for the main response peak. The decays may be used to identify the type of source, independent of the geometrical response which is dependent on the mutual coupling.

Model and Physical Conductors

Economic conductive mineral deposits have no unique feature which would make their identification a straightforward process. Most ore bodies do have conductivity contrasts and at least one dimension which is significantly small. A conductivity contrast is necessary to overcome the "skin depth" attenuation effects of conductive overburden or lateritic soils on the primary electromagnetic field (West and Macnae 1982). The recognition of dipping conductors is possible, mainly due to the double peaks encountered in an updip flight direction (Figure F1). A horizontal

mineral deposit is potentially the most difficult to select because the horizontal sheet model also applies to conductive overburden and lateritic soils. The theoretical shapes may be matched to physical-geological situations as has been done in the following summary:

a) THIN DIPPING SHEET OR PLATE:

economic - stratiform tabular ore body, dyke, vein, fault, fracture mineralization;
non economic - graphitic-carbonaceous shales, barren sulphides
cultural - some grounded power lines, fences

b) SPHERE - CYLINDER:

economic - compact massive orebody; horizontal pipe-shaped conductor
cultural - some pipelines

c) HORIZONTAL SHEET:

economic - some stratabound massive sulphides
non economic - overburden, lateritic soils
- weathered rock
- sea water or saline formations
- graphitic metasediments

d) VERTICAL STRIP (RIBBON)

economic

and

non economic - rarely encountered in nature

cultural - grounded hydro lines, lightning arrestor lines, fences

e) HORIZONTAL STRIP (RIBBON)

economic - some stratabound massive sulphides

non economic - some syngenetic mineral deposits

geological - weathering of narrow basic rock units with a high amphibolite content

cultural - grounded and interconnected fences, pipes

THE THIN DIPPING PLATE RESPONSE

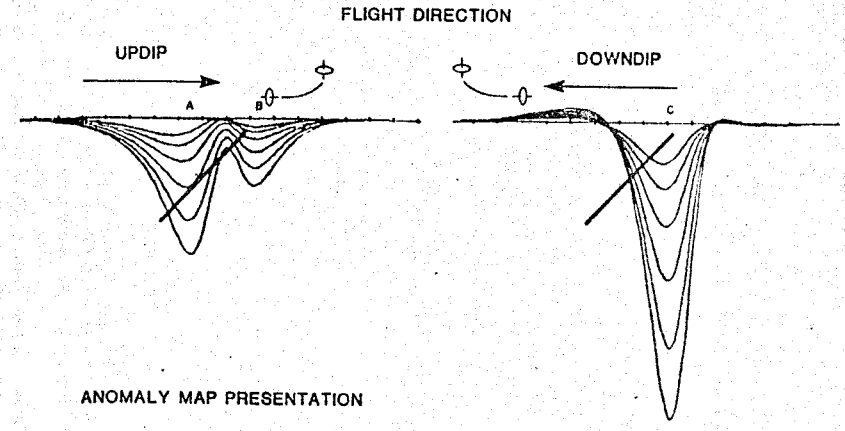

ANOMALY MAP PRESENTATION

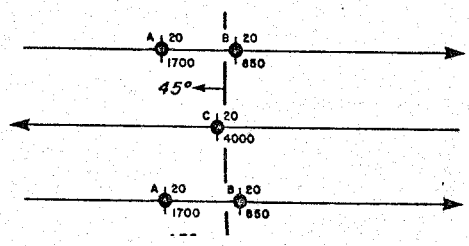

The interpreted conductor axis location varies with the source dip, conductivity, depth, thickness, depth extent and angle of intersection of the flight line to the conductor (strike direction).

THE SPHERE OR CYLINDER RESPONSE

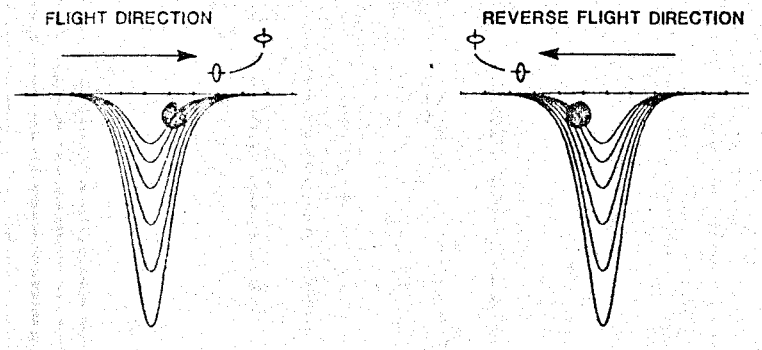

ANOMALY MAP PRESENTATION

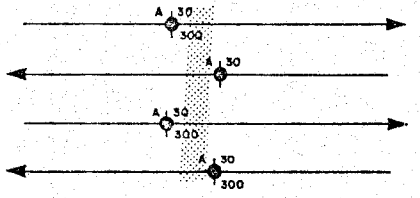

The response of a cylinder may be quite difficult to recognize from a thin strip. A cylinder or spherical model does not show a pronounced negative or upward peak following the main response. Due to the effect of the time constant of the INPUT receiver, the negative peaks which follow the theoretical response do not appear on the INPUT records (Mallick 1972, Morrison et al 1973). As the illustrations show, the sphere-cylinder response is perfectly symmetrical, but not centered over the body. The plotting position of the main peak leads the actual axis location because the most favourable mutual coupling occurs just before the transmitter coil passes the conductive body. The amplitude of the responses will be similar in both flight directions for a perfect cylinder.

THE HORIZONTAL SHEET

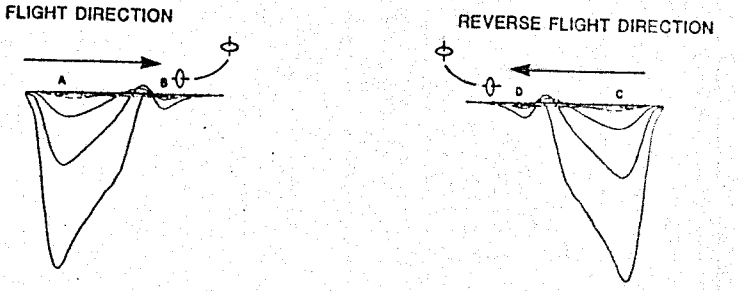

ANOMALY MAP PRESENTATION

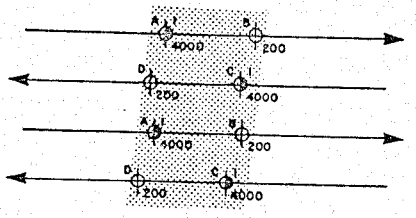

The horizontal conducting sheet has many variations but it is essentially simple to recognize. The amplitudes of the earlier channels may reach 30,000 ppm where saline solutions are present, however, horizontal sheet responses of channels 4, 5 and 6 attenuate, much faster than for a vertical or steeply dipping plate.

The edge effect is a common interpretational problem where the conductive layer has low resistivities. A secondary peak may occur as the receiver coil crosses the far sheet edge. These responses are always very sharp and often have very high apparent conductivities.

The edges of the sheet are positioned approximately at the half-peak width positions which are usually the inflection points of the profile.

The variations in plotting positions observed for dipping sheets are not as evident for the plate.

It is not unusual to see a shift in the peaks, with the latter channels migrating towards a section of improved conductance and/or increasing thickness. Another characteristic of poorly conducting sheets which respond only on channels 1 through 4 is the inversion of responses on channels 5 and 6. This is a reaction of the compensation circuits to changes in the primary field in the presence of a strong conductor and it serves no practical end except as a recognition aid.

The horizontal sheet model also applies to residual soils or laterite as well as conducting rock units. As the thin overburden situation changes to a thick overburden or two layer case and finally to a half space or a uniformly conductive earth, the responses also vary. The latter cases will have progressively broader responses which would seldom be mistaken for true discrete conductive zones.

When flight lines in opposite directions cross a conductive sheet, an asymmetric mirror image response occurs when the sheet is uniform. If there are variations in the geometry or conductance across the sheet, it may be necessary to compare responses with a shallow dipping sheet conductor to determine the effects, which would not be similar when compared with adjacent lines.

THE HORIZONTAL STRIP (RIBBON) RESPONSE

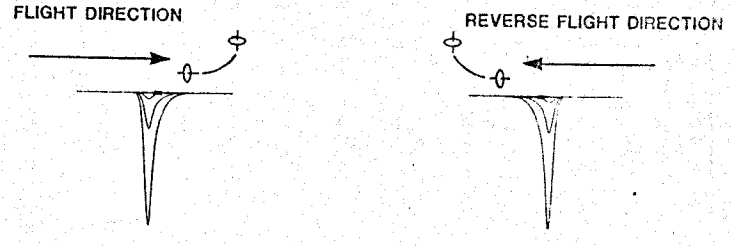

ANOMALY MAP PRESENTATION

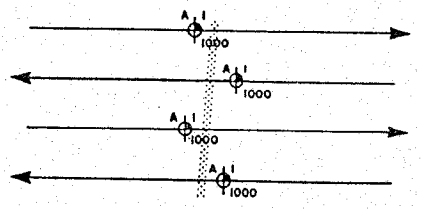

The plotting positions of the responses could easily be mistaken for a vertical plate conductor, however, careful consideration must be given to the line direction. The horizontal ribbon is a degeneration of the horizontal conducting sheet. It can be easily distinguished from a sphere or cylindrical body by its peak asymmetry, whereas the sphere model has a single symmetric main response.

THE VERTICAL STRIP (RIBBON) RESPONSE

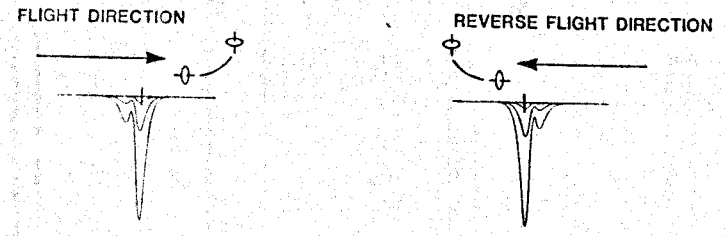

ANOMALY MAP PRESENTATION

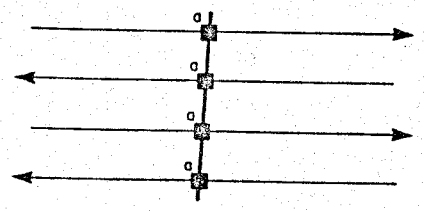

Due to the fact that this type of response is most commonly caused by fences, lightning protection lines and grounded power lines, the customary cultural presentation is a square symbol. This cultural response symbol may or may not have a power monitor (50-60 cycle) response but these will normally follow pipelines, fences, power lines, roads, railroads and other man made structures. The amplitude and apparent conductivity of such responses varies with the ground conductivity. In residual soils or conductive overburden, it is often possible to see a positive (up-dip type) peak followed by a small negative immediately before the main conductive response. The presence and amplitudes of such responses is normally very consistent. The cause of such responses is interpreted to be current gathering within the surficial sediments (West and Macnae 1982).

APPENDIX G

Quantitative Interpretation

The quantitative interpretation of the INPUT data is normally accomplished by comparing the resultant responses with type curves obtained from theoretical calculations, scale model studies and actual field measurements. A variety of results are available in literature for different conductor geometries and system configurations (see Ghosh 1972, Palacky 1974, Becker et al., 1972, Lodha 1977, Ramani 1980). They also examined the effects of varying such parameters as conductance, conductor depth, dip and depth extent. Their approach has been successfully applied in interpretation of past field surveys.

The nomograms which are currently available for the INPUT system are the Vertical Half-Plane, Homogeneous Half-Space, Thin Overburden and 135 Dipping Half-Plane nomograms. The first is particularly useful for the interpretation of vertical dyke-like conductors frequently found in the Precambrian Shield type environments. In the case of a thick, homogeneous, flat-lying (less than 30 dip) source, the Homogeneous Half-Space nomogram should be applied. While in a thin overburden or tropically weathered rock environment, the Thin Overburden nomogram may be referenced to determine the depth and conductance of the overburden (Palacky and Kadekaru, 1979).

As an example, INPUT anomalies due to vertical dyke-like conductors, are asymmetric and independent of the flight direction. Their shape is characterized by a minor first peak and a major

second peak and their channel amplitudes are a function of the conductivity-thickness product and depth of the source. Anomaly A in Figure G1 illustrates one of these responses.

The channel amplitudes of anomaly A can be used in quantitative interpretation in the following way. Their values are plotted for each of the six channels on logarithmic (5 cycles K+E 46 6213) tracing paper in a straight line using the vertical logarithmic scale in parts per million as given on the right side of Figure G2. The six channel amplitudes for anomaly A, in ppm, are 840, 540, 390, 280, 180, 120, respectively. The amplitudes are measured in ppm (1mm - 30 ppm) from the flight records with reference to the normal background levels on respective channels. Those responses which are not at least three channels or whose first channel amplitude is less than 2 mm or 60 ppm over the normal background should be discarded in the present analysis. The six points on the semi-logarithmic paper are then fitted to the curves of the vertical half-plane nomogram (Figure G2) without any rotation. Having accomplished this, the lateral placement of the plot indicates the apparent conductivity-thickness value, in siemens, and the position of the 10,000 ppm line on the logarithmic paper indicates the conductor depth, in metres. In the example shown (Figure G2), the apparent conductivity-thickness value is 31 siemens and the depth is 46 metres.

The asymmetric Tx-Rx configuration is very sensitive to changes of dip, particularly in the case of conductors dipping against the flight direction. In this circumstance, there is a change in the magnitude of the second/first peak ratio for all

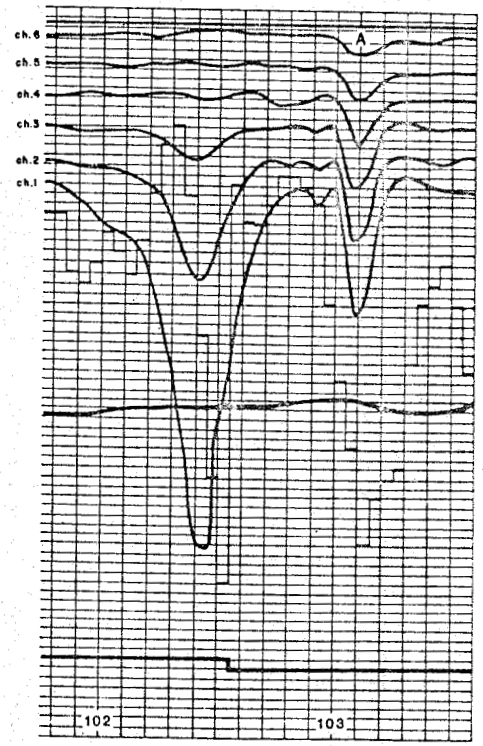

Figure G1

FIXED WING INPUT
VERTICAL HALF PLANE
CONDUCTIVITY / DEPTH NOMOGRAM

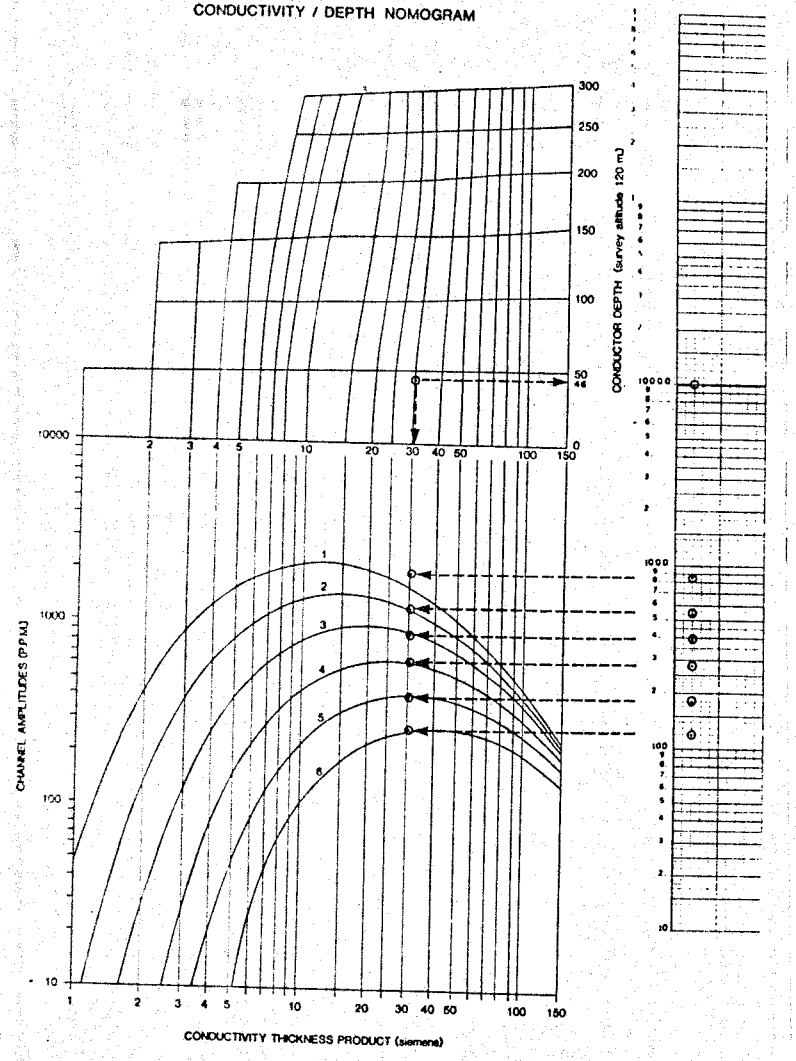

Figure G2

QUESTOR INPUT
THIN PLATE DIP ESTIMATION
and
AMPLITUDE NORMALIZATION GRAPH

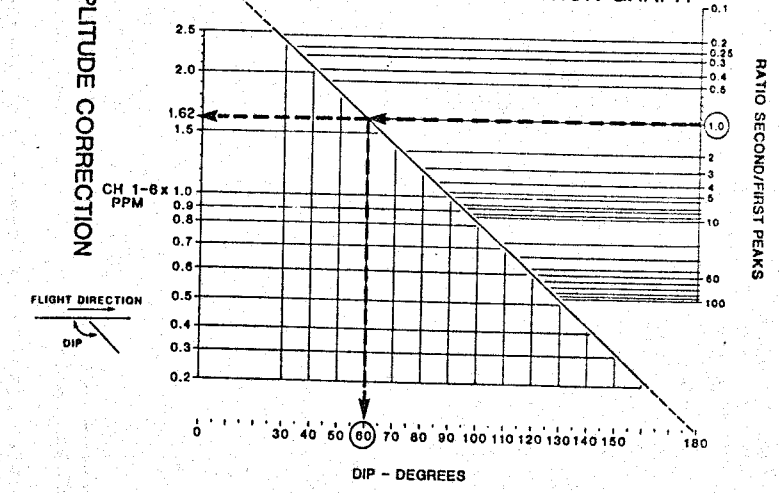

Figure G3

channels. The ratio of the amplitudes of the two peaks is a function of dip. The dip should be the first parameter determined in the quantitative interpretation of a dipping conductor. Before the amplitude is further used for an estimate of conductivity-thickness and depth, it must be normalized to a dip of 90^{o}. This correction is performed by means of the Thin Plate Dip Estimation and Amplitude Normalization Graph, Figure G3.

From the graph, it can be seen that a vertical dyke conductor should have a second/first peak ratio of approximately 6, i.e., that the first peek will have 16% of the amplitude of the second peak. In the case of anomaly A, this condition is true. Conversely, should the dyke dip at 60^{o}, the ratio will decrease to 1.0. Thus, the dip of a conductor can be estimated from the peak ratios of channel two by using the graph in Figure G3.

An example of amplitude correction determination is shown in Figure G3. A dipping conductor has an up-dip second-first peak ratio of 1.0 i.e., that the channel amplitudes of the minor first peak and major second peak of channel two are equal. Taking this ratio of 1.0 and applying the graph, we obtain a dip of 60^{o} for the conductor and an amplitude correction of approximately 1.62. Consequently, the correction factor is applied to the six channel amplitudes of the associative down-dip response. This response is then fitted to the vertical half-plane nomogram for the determination of its apparent conductivity-thickness value and depth. It should be mentioned that without the dip correction, the depth would be overestimated.

An alternate method for estimating the dips of longer, tabular conductors, utilizes the peak amplitudes on adjacent lines, see Figure G4. It is especially useful in multiple conductive zones where the up-dip responses may be obscured or yield false values due to the superposition of other nearby anomalies.

Note that the depth determination is made with the assumption that the aircraft is at 120 metres above the ground surface at the time of measurement. If the aircraft is above or below the altitude of 120 metres, the depth determination can be corrected by respectively, subtracting or adding the difference in altitude, within limits.

The homogeneous half-space, thin overburden and the dipping half-plane 135^{o} nomograms are used in the same fashion as that described above for the vertical half-plane.

To estimate the apparent strike length of a conductor, the ends of the conductive trend must be determined. Modelling has shown that the conductor ends are delineated by INPUT responses having channel amplitudes not less than 40% of those typical for the conductor. Responses with less than that of 40% are attributive to lateral coupling effects and are not considered as intercepts of the conductor. This is especially true for conductors of higher conductivity. Subsequently, the strike length of a conductor is equal to the distance between those responses representing the ends of the conductor.

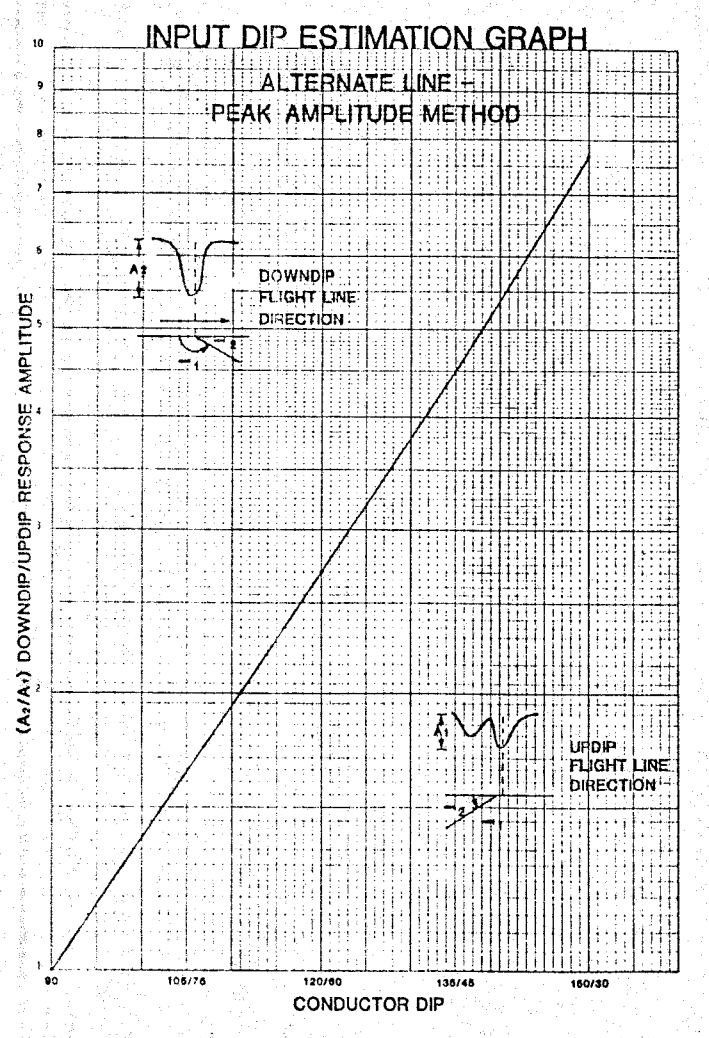

Figure G4

APPENDIX H

Bibliography

Barringer, A.R., 1962, The INPUT Airborne Electrical Pulse Prospecting System: Min. Cong. J., volume 48, page 49-52;

Barringer Research Limited, 1962, Method and Apparatus for the Detection of Ore Bodies: United States Patent Office: 3.020,471;

Barringer Research Limited, The Quantitative Interpretation of Airborne INPUT Electromagnetic Data: Barringer Research Technical Note;

Becker, A., 1969, Simulation of Time-Domain, Airborne Electromagnetic System Response: Geophysics, volume 24, page 739-752;

Becker, A., Gavreau, D., and Collett, L.S., 1972, Scale Model Study of Time-Domain Electromagnetic Response of Tabular Conductors: CIM Bull., volume 65, number 725, page 90-95;

Dyck, A.V., Becker A., and Collett, L.S., 1974, Surficial Conductivity Mapping with the Airborne INPUT System: CIM Bull., volume 67, number 744, page 104-109;

Ghosh, M.K., and West, G.F., 1971, EM analog model studies: Norman Paterson and Associates, Toronto;

Lazenby, P.G., 1972, Examples of Field Data Obtained with the INPUT Airborne Electromagnetic System: Questor Surveys Limited;

Lazenby, P.G., 1972, New Developments in the INPUT Airborne EM System: CIM Bull., volume 66, number 732, page 96-104;

Mallick, K., 1972, Conducting Sphere in Electromagnetic INPUT Field: Geophysical Prospecting, volume 20, page 293-303;

Macnae, James C., 1979, Kimberlites and Exploration Geophysics: Geophysics, volume 44, number 8, page 1395-1416;

Mishra, D.C., Murthy, K.S.R., and Narain, H., 1978, Interpretation of Time-Domain Airborne Electromagnetic (INPUT) Anomalies: Geoexplor., volume 16, page 203-222;

Morrison, H.F., Phillips, R.J., and O'Brien, D.P. 1969, Quantitative Interpretation of Transient Electromagnetic Fields Over a Layered Half-Space: Geophys. Prosp. volume 7, page 82-101;

Nelson, P.H., and Morris, D.B., 1969, Theoretical Response of a Time Domain, Airborne, Electromagnetic System: Geophysics, volume 34, page 729-738;

Nelson, P.H., 1973, Model Results and Field Checks for a Time-Domain, Airborne EM System: Geophysics, volume 38, page 845-853;

Palacky, G.J., and West, G.F., 1974, Computer Processing of Airborne Electromagnetic Data: Geophysical Prospecting 22, page 490-509;

Palacky, G.J., and West, G.F., 1973, Quantitative Interpretation of INPUT AEM measurements: Geophysics, volume 38, page 1145-1158;

Palacky, G.J., 1974, The Atlas of INPUT Profiles: B.R.L. Toronto, page 37;

Palacky, G.J., 1975, Interpretation of INPUT Measurements in Areas of Conductive Overburden: Geophysics, volume 40, page 490-502;

Palacky, G.J., 1976, Use of Decay Patterns for the Classification of Anomalies on Time-Domain AEM Measurements: Geophysics, volume 41, page 1031-1041;

Palacky, G.J., 1977, Selection of a Suitable Model for Quantitative Interpretation of Towed-Bird AEM Measurements: Geophysics, volume 43, number 3, page 576-587;

Palacky, G.J., and Kadekaru, K., 1979, Effect of Tropical Weathering on Electrical and Electromagnetic Measurements: Geophysics, volume 44, page 21-38;

Palacky, G.J., and Sena, F.O., 1979, Conductor Identification in Tropical Terrains - Case Histories from the Itapicuru Greenstone Belt, Bahia, Brazil: Geophysics, volume 44, page 1931-1962;

Questor Surveys Limited, 1974, Airborne INPUT Responses: Questor Surveys Limited, Mississagua, Ontario;

Verma, S.K., 1975, Resolution of Responses due to Conductive Overburden and Ore-Body through Time-Domain EM Measurements: Geophysical Prospecting, volume 23, page 292-299.

NAME : MARCEL H. KONINGS

OCCUPATION : Senior Geophysicist

EDUCATION : B.A.Sc., Geological Engineering.
University of Toronto, Toronto, Ontario.

PROFESSIONAL AFFILIATIONS : Society of Exploration Geophysicists (SEG)

Canadian Exploration Geophysical Society (KEGS)

Association of Professional Engineers of the Province of Ontario (APEO).

EXPERIENCE :

1980 Questor Surveys Limited.
Senior Geophysicist.
Responsible for supervision, reporting and interpretation of INPUT and magnetometer survey data.

1981-82 Project Manager/Geophysicist
Mexico magnetics/radiometrics project including field operations, data compilation and interpretation.

1982 Project Manager/Geophysicist.
Brazil INPUT surveys. Responsibilities included field operations, data compilation and interpretation at survey locations.

1976 Shell Canada Resources.
Project Geophysicist.
Duties included supervision of EM, IP, gravity and magnetic surveys as well as interpretation. Geophysical surveys and interpretation resulted in the successful drilling of the East Kemptville tin deposit.

1975 Prospection Limited.
Contract Geophysicist.
Based in the Sultinate of Oman.
Responsibilities included evaluation of INPUT survey results, supervision of geophysical field parties and interpretation of ground transient electromagnetics, magnetics and gravity. Two new deposits were delineated.

1975 Crone Geophysics Limited.
Contract Geophysicist.
Responsible for gravity and elevation surveys, data reduction and interpretation.

1974 Amoco Canada Petroleum Co. Ltd.
Project Engineer.
Involved in mineral exploration programs from initial INPUT surveys through drilling.
Part of Detour Lake discovery team.

1972 Amoco Canada Petroleum Co. Ltd.
Geological and geophysical surveying.

1971 New Jersey Zinc Exploration Co.
Geophysical Operator.

COUNTRIES WORKED IN : Canada, Oman, Mexico and Brazil.

LANGUAGES SPOKEN : English, Dutch, and a working knowledge of French, Portuguese, Spanish

PASSPORT # : MA 691 641 Expires December 30, 1985.

CITIZENSHIP : Canadian

DATE OF BIRTH : August 22, 1951

PLACE OF BIRTH : Geleen, Netherlands

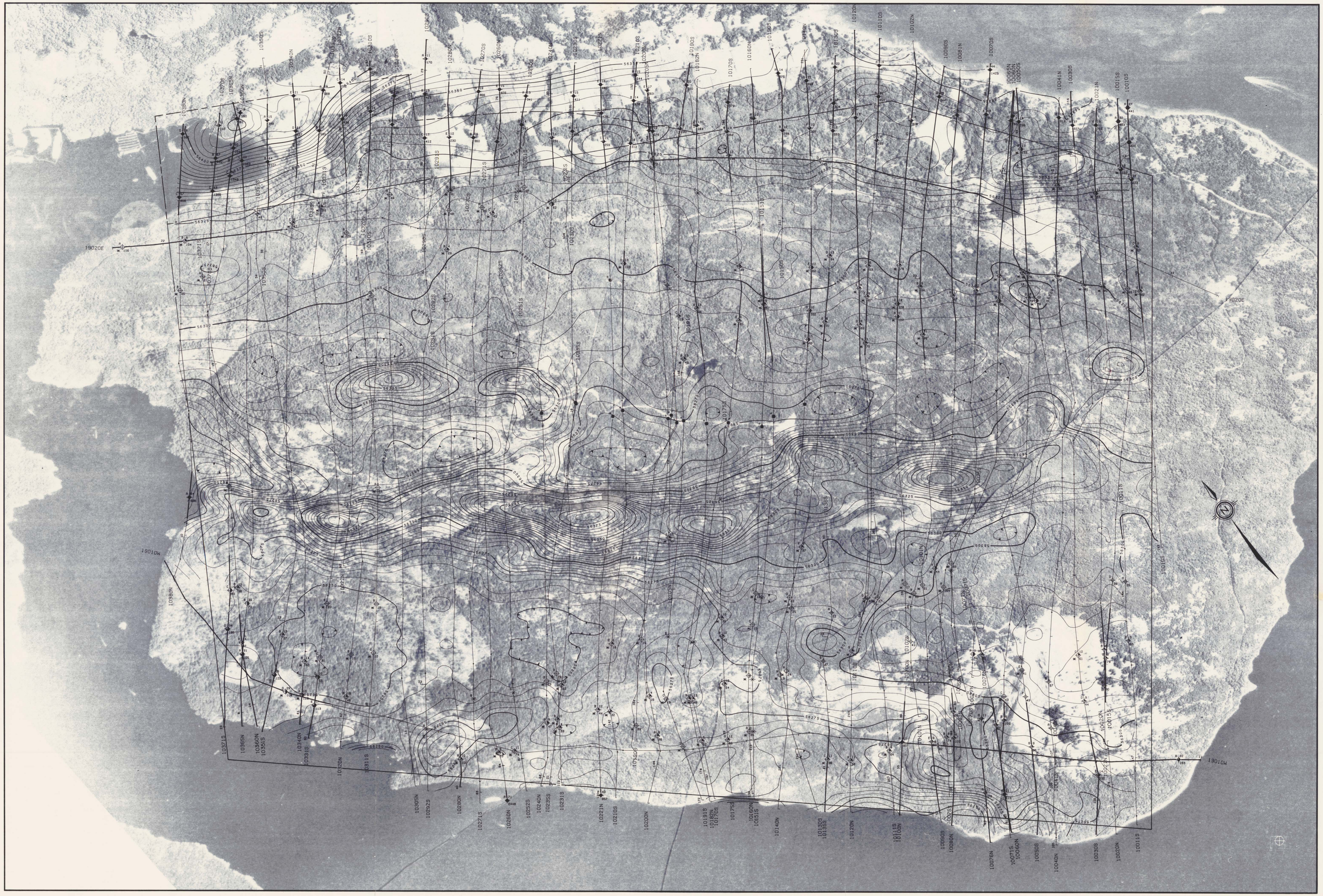

INPUT® — Helicopter Vertical Axis Coil 2ms PULSE

SURFICIAL RESPONSE	UP-DIP PEAK RESPONSE	BEDROCK RESPONSE	DECAY INTERVAL CLASSIFICATION
			1 Channel (300 microseconds)
			2 Channel (500 microseconds)
			3 Channel (800 microseconds)
			4 Channel (1200 microseconds)
			5 Channel (1700 microseconds)
			6 Channel (2300 microseconds)

Culture Response

50 Associated Magnetic Response

Channel 1 Half-Peak Width

Anomaly Letter — B

Apparent Conductivity Width (siemens) (N.C. - No Calculation) — 5

Poorly Defined Response — *

Ch. 2 Amplitude (p.p.m.) — 1800

MAGNETIC CONTOURS

5 Gamma Contour Line

25 Gamma Contour Line

100 Gamma Contour Line

Magnetic Depression

1 Gamma = 1 Nanotesla in SI Units

GEOLOGICAL BRANCH
ASSESSMENT REPORT

13,375

PART 2 OF 2

Note-
Original Survey Boundary
Survey Boundary Extension

Representative INPUT® Magnetometer and Altimeter Recording

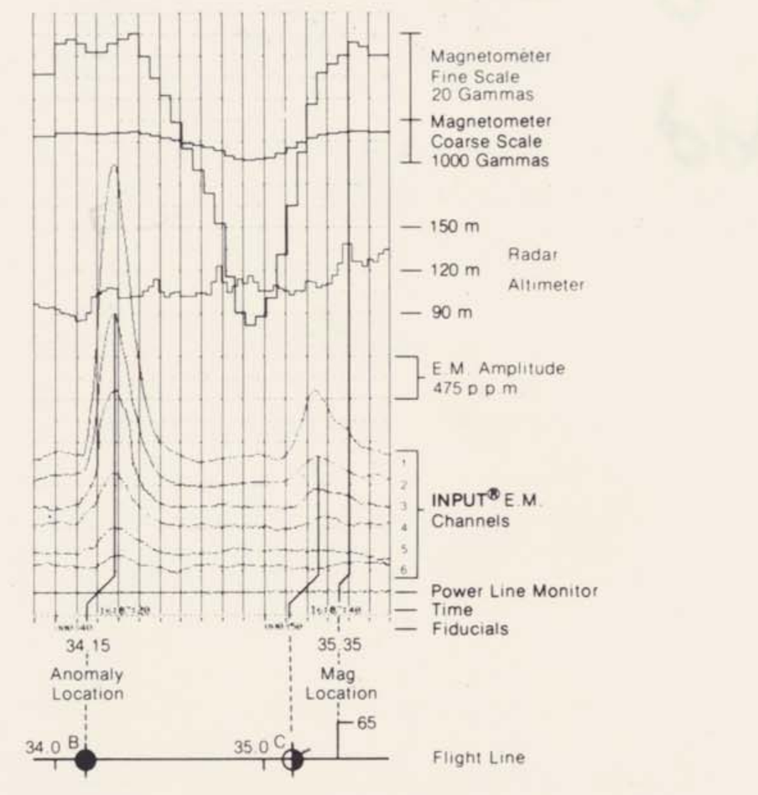

DESCRIPTIVE NOTES

The aircraft is equipped with the Barringer/Questor Mark VI INPUT* airborne E.M. System and the Sonotek PMH 5010 Proton Precession Magnetometer and Sonotek SDS-1200 Series Data Acquisition System. The INPUT* system will respond to conductive overburden and near-surface horizontal conducting layers in addition to bedrock conductors. Discrimination of conductors is based on the rate of transient decay, magnetic correlation and the anomaly shape, together with the conductor pattern and topography.

* Registered Trade Mark of Barringer Research Limited

INTERPRETATION REFERENCES

Becker, A., Gauvreau, C., and Collett, L.S.
1972: Scale Model Study of Time Domain Electromagnetic Response of Tabular Conductors; Canadian Mining and Metallurgical Bulletin, Volume 65, No. 725, p. 90-96.

Dyck, A.V., Becker, A., and Collett, L.S.
1974: Surficial Conductivity Mapping with the Airborne INPUT* System; Canadian Mining and Metallurgical Bulletin, Volume 67, No. 744, p. 104-109.

Lazenby, P.G.
1973: New Developments in the INPUT* Airborne E.M. System; Canadian Mining and Metallurgical Bulletin, Volume 66, No. 732, p. 96-104.

Nelson, Philip, H.
1973: Model Results and Field Checks for a Time-Domain Airborne E.M. System; Geophysics, Volume 38, No. 5, p. 845-853.

Palacky, G.J., and West G.F.
1974: Computer Processing of Airborne Electromagnetic Data; Geophysical Prospecting, Volume 22, No. 3, p. 490-509.

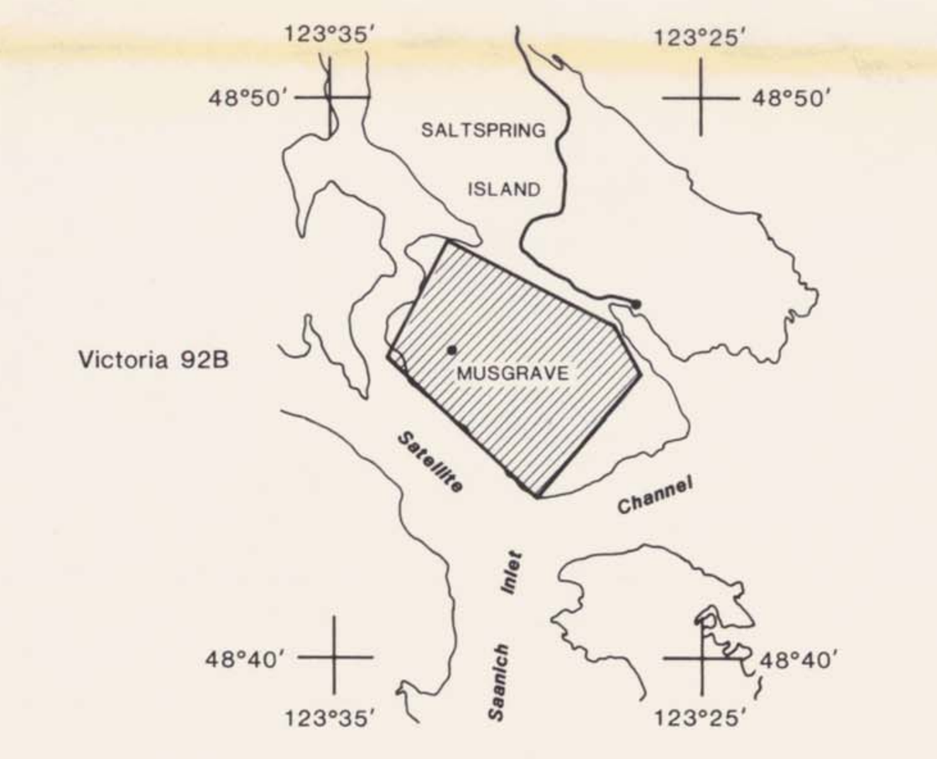

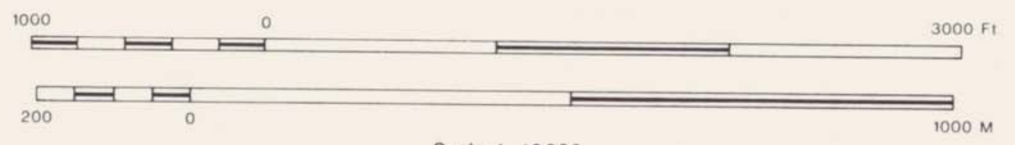

Scale 1: 10000

AIRBORNE MK VI INPUT® SURVEY
TOTAL MAGNETIC INTENSITY SURVEY

Kidd Creek Mines Limited

SALTSPRING ISLAND

Province of BRITISH COLUMBIA

FILE NO.	SHEET NO.	DATE	COMPILED BY
26H19	1 of 1	June 1984	Questor Surveys Limited

Questor Surveys Limited
Mississauga Ontario Canada

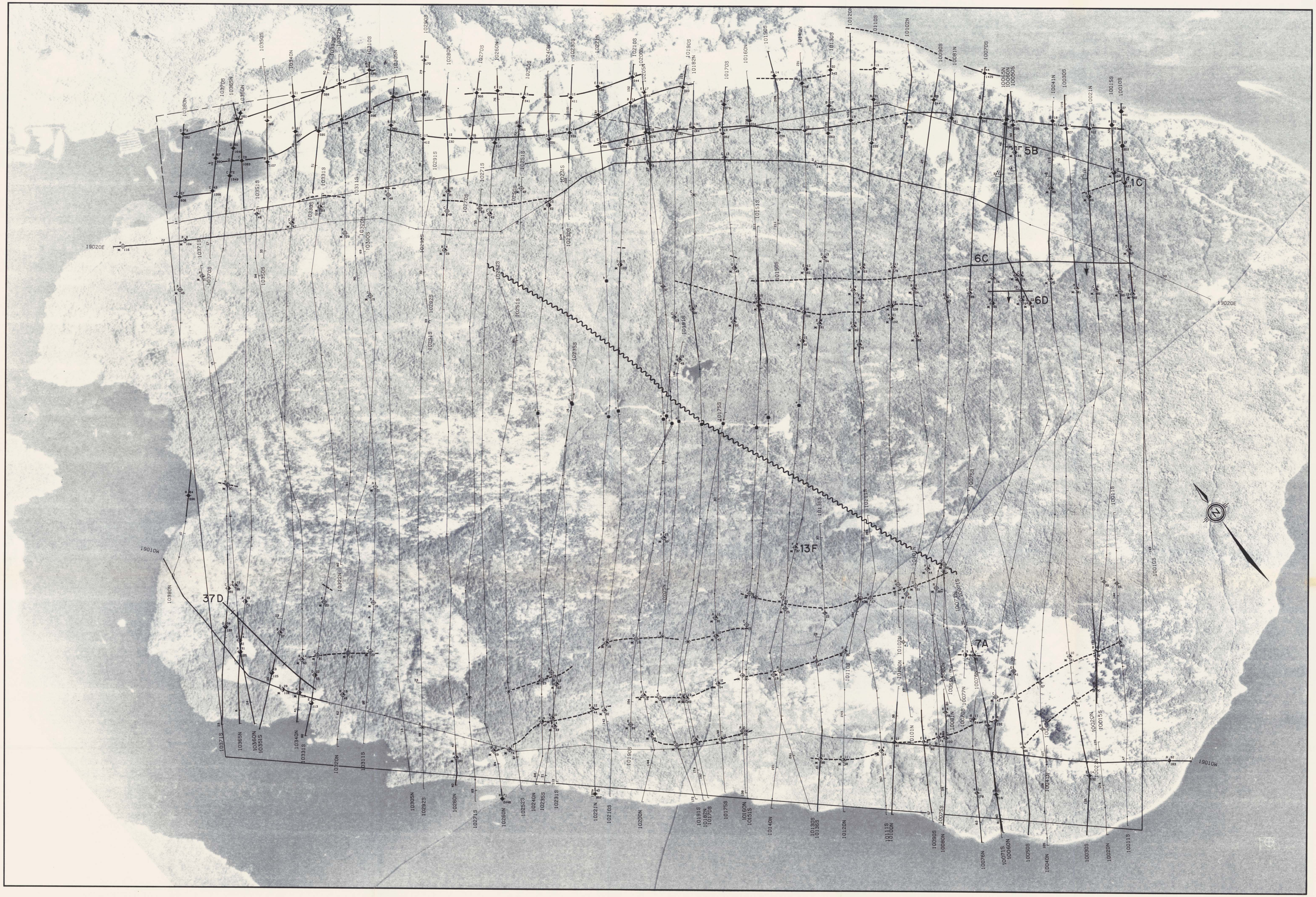

INPUT® — Helicopter Vertical Axis Coil 2ms PULSE

SURFICIAL RESPONSE	UP-DIP PEAK RESPONSE	BEDROCK RESPONSE	DECAY INTERVAL CLASSIFICATION
			1 Channel (300 microseconds)
			2 Channel (500 microseconds)
			3 Channel (800 microseconds)
			4 Channel (1200 microseconds)
			5 Channel (1700 microseconds)
			6 Channel (2300 microseconds)

Culture Response

50 Associated Magnetic Response

A Channel 1 Half-Peak Width

Anomaly Letter — B 5 1800 — Apparent Conductivity Width (siemens) (N.C. - No Calculation); Poorly Defined Response; Ch. 2 Amplitude (p.p.m.)

GEOLOGICAL BRANCH ASSESSMENT REPORT

13,375

PART 2 OF 2

INTERPRETATION

20 Conductor Axis, with reference number good definition)

20 Conductor Axis, with reference number (poor definition)

Vertical Conductor

Conductor Dip (magnitude and direction known)

Conductor Dip (direction known)

20 Selected Zone, with reference number

Conductive Zone

Fault Zone

Note- Original Survey Boundary; Survey Boundary Extension

Representative INPUT® Magnetometer and Altimeter Recording

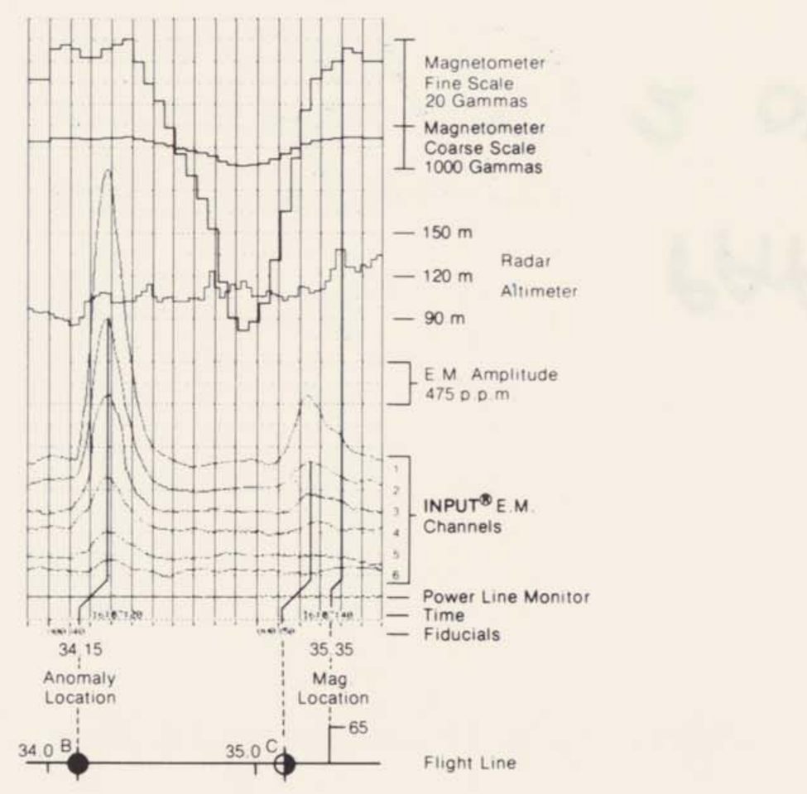

DESCRIPTIVE NOTES

The aircraft is equipped with the Barringer/Questor Mark VI INPUT* airborne E.M. System and the Sonotek PMH 5010 Proton Precession Magnetometer and Sonotek SDS-1200 Series Data Acquisition System. The INPUT* system will respond to conductive overburden and near-surface horizontal conducting layers in addition to bedrock conductors. Discrimination of conductors is based on the rate of transient decay, magnetic correlation and the anomaly shape, together with the conductor pattern and topography.

* Registered Trade Mark of Barringer Research Limited

INTERPRETATION REFERENCES

Becker, A., Gauvreau, C., and Collett, L.S.
1972: Scale Model Study of Time Domain Electromagnetic Response of Tabular Conductors; Canadian Mining and Metallurgical Bulletin, Volume 65, No. 725, p. 90-96.

Dyck, A.V., Becker, A., and Collett, L.S.
1974: Surficial Conductivity Mapping with the Airborne INPUT* System; Canadian Mining and Metallurgical Bulletin, Volume 67, No. 744, p. 104-109.

Lazenby, P.G.
1973: New Developments in the INPUT* Airborne E.M. System; Canadian Mining and Metallurgical Bulletin, Volume 66, No. 732, p. 96-104.

Nelson, Philip, H.
1973: Model Results and Field Checks for a Time-Domain Airborne E.M. System; Geophysics, Volume 38, No. 5, p. 845-853.

Palacky, G.J., and West G.F.
1974: Computer Processing of Airborne Electromagnetic Data; Geophysical Prospecting, Volume 22, No. 3, p. 490-509.

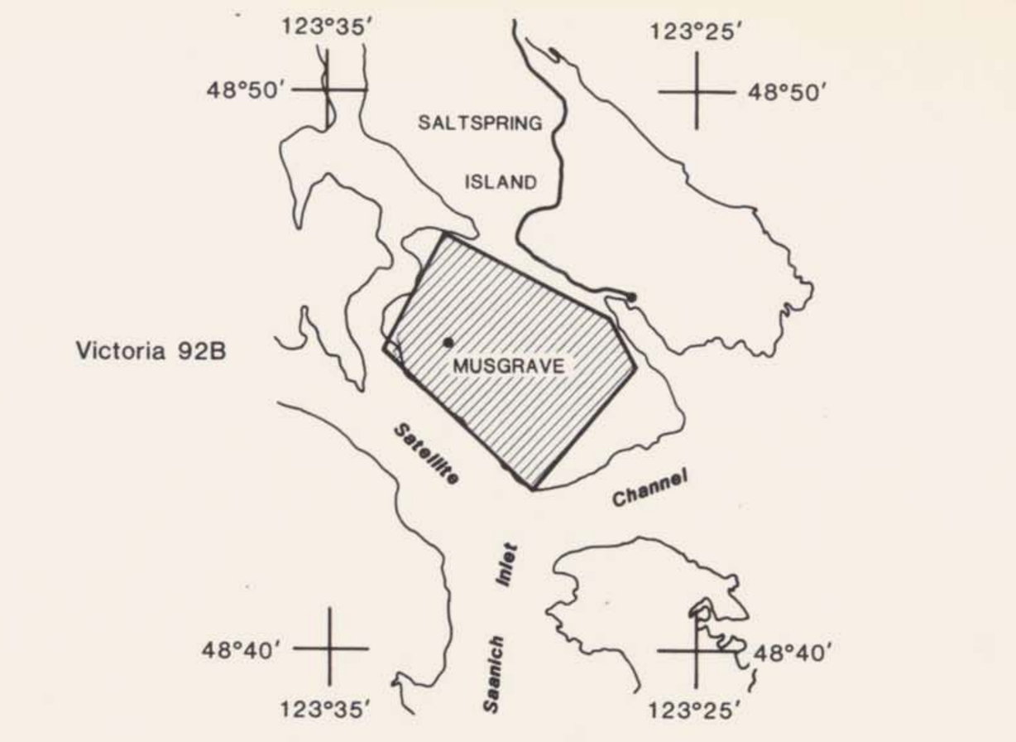

1000 0 3000 Ft.

200 0 1000 M

Scale 1: 10000

AIRBORNE MK VI INPUT® SURVEY

Kidd Creek Mines Limited

SALTSPRING ISLAND

Province of BRITISH COLUMBIA

FILE NO.	SHEET NO.	DATE	COMPILED BY
26H19	1 of 1	June 1984	Questor Surveys Limited

Questor Surveys Limited
Mississauga Ontario Canada